HOKKAIDO UNIVERSITY

Title	Mitochondrial Visualization in Rice Blast Fungus and its Application to 3D Observation, Quantification, and Distribution Analysis
Author(s)	Muhammad Akhid Syib'li
Degree Grantor	北海道大学
Degree Name	博士(農学)
Dissertation Number	甲第13919号
Issue Date	2020-03-25
DOI	https://doi.org/10.14943/doctoral.k13919
Doc URL	https://hdl.handle.net/2115/94542
Type	doctoral thesis
File Information	Muhammad_Akhid_Syib'li.pdf

Hokkaido University Collection of Scholarly and Academic Papers : HUSCAP

Mitochondrial visualization in rice blast fungus and its application to 3D observation, quantification, and distribution analysis

（イネいもち病菌のミトコンドリアの可視化とその３次元観察，定量及び分配解析への応用）

Ph.D Dissertation

(The Special Postgraduate Program in Bio-system Sustainability)

Muhammad Akhid Syib'li



Laboratory of Applied Microbiology
Division of Applied Bioscience
Graduate School of Agriculture
Hokkaido University

Sapporo, Japan
January 2020

Mitochondrial Visualization in Rice Blast Fungus and its Application to 3D Observation, Quantification, and Distribution Analysis

（イネいもち病菌のミトコンドリアの可視化とその３次元観察，定量及び分配解析への応用）

Muhammad Akhid Syib'li

Submitted to the Graduate School of Agriculture

Hokkaido University

January 2020

In Partial Fulfillment of the Requirement for the Degree of

Doctor of Philosophy in Applied Microbiology

TABLE OF CONTENT

Table of content i

List of tables .....

List of figures .....

CHAPTER 1 - **Introduction**

1.1 Rice blast disease dispersion and conidia formation 2

1.2 Septal pore in *Pyricularia*, organelle migration and cells communication 3

1.3 Conidiophore structure and organelle migration into conidia 4

1.4 Mitochondrial behavior and fungicide 5

1.5 Quinone outside Inhibitor (QoI) and pathogenic fungal resistance 7

CHAPTER 2 – **Visualizing mitochondria of *Pyricularia* oryzae**

2.1 Introduction 15

2.2 Materials and Methods 17

2.3 Result 19

2.3.1 The use of Calcofluor white for staining conidial wall 19

2.3.2 The use of MitoTracker to confirm (*Cit*A)-GFP for staining Mitochondria 19

2.3.3 Identification of the appropriate timing of conidiation 20

2.3.4 Analysis of Conidial mitochondrial 3D visualization 20

2.4 Discussion 22

CHAPTER 3 – **Quantification of conidial mitochondrial volume using MitoGraph software**

3.1 Introduction 31

3.2 Materials and Methods 32

3.3 Result and Discussion..... 34

3.3.1 Modification of macro CropCells.ijm 34

3.3.2 Run MitoGraph..... 35

CHAPTER 4 – **Visualization of mitochondrial dynamics during conidia formation using slide culture-confocal microscopy**

4.1 Introduction 46

4.2 Materials and Methods 46

4.3 Result and Discussion..... 48

4.3.1 Conidia formation and time-lapse observation 48

4.3.2 Mitochondrial dynamic during conidia development 48

CHAPTER 5- **General Discussion**..... 70

REFERENCES 73

ACKNOWLEDGMENT 81

LIST OF FIGURES

Fig 1.1 The symptom of rice blast fungus and conidial dispersal illustration..... 10

Fig 1.2 Development of conidia in three isolates of *P. oryzae*..... 11

Fig 1.3 Conidia of *P.oryzae*..... 12

Fig 1.4 Septal pore and woronin bodies in ascomycete fungi,
Zymoseptoria tritici 13

Fig 1.5 Schematic representation of the mitochondrial electron transport system.... 14

Fig 2.1 Conidia of *P. oryzae*. 22

Fig 2.2 Conidia with 3 cells and mitochondrial appearance..... 23

Fig 2.3 Identification of the appropriate timing to observe conidiation..... 24

Fig 2.4 Conidia with different number of cells 26

Fig 2.5 Mitochondria morphology in each type of conidia. 27

Fig 2.6 Mitochondria morphology in the conidia and hyphae 29

Fig 3.1 The work flow of the study of conidial mitochondrial
volume measurement..... 37

Fig 3.2 MitoGraph Software and the supporting software 38

Fig 3.3 The display of GenerateFramesMaxProjs.ijm and CropCell.ijm..... 39

Fig 3.4 The workflow of MitoGraph software 40

Fig 3.5 The display of MitoGraph output and Short explanation..... 41

Fig 3.6 Relationship between mitochondrial volume (based on voxel)
and conidial length 42

Fig 3.7 Relation between mitochondrial volume (based on length)
And conidial length..... 43

Fig 3.8 Distribution of mitochondrial volume (Based on voxel) 44

Fig 3.9 Distribution of mitochondrial volume (Based on length) 45

Fig 4.1 Modified Slide Culture Technique 51

Fig 4.2 Conidia development from conidiophore..... 52

Fig 4.3 Time lapse of mitochondrial behavior in the hyphae of *Pyricularia oryzae*..... 57

Fig 4.4 Complete conidia and mitochondria development..... 58

Fig 4.5 The changes in mitochondrial volume during conidia development (sample1)..... 61

Fig 4.6 Incomple conidia and mitochondria development 62

Fig 4.7 The changes in mitochondrial volume during conidia development (Sample 2)..... 69

LIST OF TABLES

Table 1. Category of Mitochondrial morphology of *P. oryzae* 29

Mitochondrial visualization in rice blast fungus and its application to 3D observation, quantification, and distribution analysis

(イネいもち病菌のミトコンドリアの可視化とその３次元観察，定量及び分配解析への応用)

Pyricularia oryzae is a multi-host pathogenic fungus that causes rice blast disease, one of the most serious threats to our global food security. Recently, emergence and spread of QoI fungicide resistance is a serious problem in many plant pathogens including *P. oryzae*. This QoI fungicide targeting cytochrome b in mitochondria and affect respiratory system to kill the pathogen. QoI resistance is caused by a base substitution in cytb gene in mitochondria DNA. Conidia of *P. oryzae* are important for the spread of the pathogen. Therefore, for the elucidation of the rapid spread of QoI resistance in the natural population of *P. oryzae*, it is necessary to analyze the dynamics of mitochondria, especially during conidia formation. In this study, visualization of mitochondria by GFP was attempted. In addition, the technique was utilized for three-dimensional observation, quantification, and distribution to conidia.

1. Visualizing mitochondria in *Pyricularia oryzae* during conidia development with Citrate Synthase-GFP fusion protein

In order to visualize mitochondria, *P. oryzae* was transformed using citrate synthase (CitA)-GFP fusion protein. The vector was constructed by fusing GFP gene to N-terminal part of cintrate synthase, which produced in cytosol, and then transferred to mitochondria. The localization of GFP in mitochondria was confirmed by colocalization of GFP with mitochondria specific MitoTracker Red under fluorescence microscopy. Then

appropriate culture method for the observation of conidia development was investigated using the transformant. It is revealed that after 36 hours of incubation on oatmeal agar, conidia with one cell, two cells and three cells were harvested, and categorized them as baby conidia, young conidia, and matured conidia, respectively. 3D visualization of the conidial mitochondria in the transformant was performed with laser-scanning confocal microscopy and computer analysis with Las X software. The result indicated that mitochondria could be distributed into baby conidia as a dot and develop to a network as aging of conidia.

2. Quantification of Conidial Mitochondrial Volume using software MitoGraph

MitoGraph is an automated image processing software dedicated to calculating the volume of three-dimensional organelles and intracellular structures in live cells. In this study, this software was used to measure mitochondrial amount of randomly-collected baby, young until matured conidia as 3 dimensional-object, and characterize further the mitochondria development. Analysis of the conidial mitochondrial volume against conidial length showed that increase of mitochondrial volume did not correlated with the cellular size, different from the case of *Saccharomyces cerevisiae*. This observation indicated that cellular growth and mitochondrial growth were not synchronized. However, there remained a strong possibility of the the result was affected by the timing of conidia harvest. Continuous observation of the conidial development from conidiophore with the GFP-stained mitochondria was required for further characterization of mitochondria dynamics in the developing conidia.

3. Visualization of mitochondrial dynamics during conidia formation using slide culture-confocal microscopy

The slide culture method for conidia formation on a filter paper was established. After incubation for four days, conidia formation could be observed simultaneously under fluorescence microscopy. This observation revealed that duration of conidia development from conidiophore was about 2.5 hours. By further observation under confocal microscopy with time-lapse recording, this method will give the opportunity to see mitochondrial behavior in the hyphae and also through the acquisition of z stack images of conidial mitochondria, measurement of the mitochondrial volume for their every stage could be conducted.

Taken together, this thesis established the observation method of mitochondria in living cells in *P. oryzae*. In addition, it also revealed that basic mitochondria dynamics in hyphae and conidia of the rice blast fungus. These knowledges should contribute to further understanding of mitochondria distribution and inheritance in *P. oryzae*, which is an important key to control the spread of QoI fungicide resistance.

Chapter 1

Introduction

Pyricularia oryzae (teleomorph: *Magnaporthe oryzae*) is a filamentous ascomycetes fungus that is destructive to cereal plants that can destroy crop yield massively. This pathogen, well known as a rice blast fungus, is also a deadly plant pathogen for rice plant and a serious threat to our global food security. Every year it is capable of causes economic damage to the rice until about $66 billion, which is equal to give enough food for 60 million people (Pennisi, 2010).

As we know, almost all Asian people depend on rice consumption, but many arable lands have changed their status to become housing and industrial areas. This phenomenon also shows an increase in the human population, which inevitably continues to require the fulfillment of suitable food needs. So, the problem of the rice blast fungus attack adds to the possibility of reduced crop yield will have always been a hot topic of research because of its extraordinary destructive power. The example in 2001-2005, there are 5.7 hectares of rice devastated in Korea, Japan, China, Vietnam, and the United States (Wilson and Talbot, 2009).

Recently, emergence and spread of QoI fungicide resistance is a serious problem in many plant pathogens including *P. oryzae*. This QoI fungicide cytochrome b in mitochondria and affect respiratory system to kill the pathogen. QoI resistance is caused by a base substitution in *cytb* gene in mitochondria DNA. Conidia of *P. oryzae* are important for the spread of the pathogen. Therefore, for the elucidation of the rapid spread of QoI resistance in the natural population of *P. oryzae*, it is necessary to analyze the dynamics of mitochondria, especially during conidia formation. In this study,

visualization of mitochondria by GFP was attempted. In addition, the technique was utilized for three-dimensional observation, quantification, and distribution analysis to conidia.

1.1 Rice blast disease dispersion and conidia formation

Conidia can spread and infect other healthy plants with help from wind and rain. So, the increase of conidia concentration in the air will cause the intense of the lesion because of conidial infection (Pinnschmidt et al. 1993). Rice blast disease usually outbreak mainly when the rainy season or transition to the rainy season comes (Asibi et al. 2019).

Conidia of *P. oryzae* that spread in the air can adhere to the hydrophobic surface of a rice leaf surface. When the environment is suitable, they will start to form germ tubes with short distance and differentiating into a specialized, domed-shaped cell called an appressorium for penetration (Lee and Dean, 1994). After penetration, the primary hyphae that are produced will massively develop until causing severe infections in the rice plants and cause necrotrophic symptoms on the leaf surface (Ebbole, 2007).

The rice blast fungus attack has a unique pattern of symptoms and is easily recognized. The characteristic symptoms of the vegetative stage are the lesions with spindles and the darker gray lesions color at the center surrounded by orange line boundaries (Figure 1A). While attacks on the generative stage show blackish gray with fractures on the panicle axis (Figure 1B), fungal attacks in the panicle axis usually are called as rotten neck or neck blast. This infection can be very devastative because they cause the failure of the seed to maturate (TeBeest et al. 2007).

If we look deeper into this symptom, many conidia will be found ready to dispatch (Wilson and Talbot, 2009). During plant infection, *P. oryzae* also form conidia on the

leaf surface, make this disease become contagious. The formation of the conidia requires a supportive environment such as humid conditions, aeration and light (Lee et al. 2006; Leach, 1980), so that the fungus can produce a lot of conidia to infect other healthy plants and cause huge damage in the paddy field area.

Rao and Jesudhas (1982) observe conidia development among 23 isolates of *Pyricularia*. Conidia formation was started with a protuberance that arose on the conidiophore tips. The protrusion was a narrow constriction structure, after that the fungus develops a very small conidium (budding). With the increase of the age, the conidium will become bigger and form septum until conidium has three cells. Conidia with three cells can be indicated as matured conidia. Therefore, There are three form of conidia, such as conidia without septum (one cell), conidia with one septum (two cells) and conidia with two septa (three cells) (Kim and Lee, 2012).

1.2 Septal pore in *Pyricularia*, organelle migration and cells communication

Cells of *P. oryzae* usually are cut-off by septa in the hyphae or the conidia (Bussaban et al. 2005). In the middle of the septum of ascomycete fungi, there is a septal pore. It collaborated with specialized organelle, called woronin bodies (WB) (Fig 4.). Both of them have a function in regulating organelle flow from one to another cell (Steinberg et al. 2017a). A study from Jones et al. (2016) showed that during the invasion of rice cell and nuclear division, there is an event of the septal pore with the closed condition. After nuclear was inherited to the young generation, septal pore return to be opened. In general, septa arose after young hyphae or conidia wholly formed. However, in another strain septa are able to occur, even before conidia have not entirely developed (Rao and Jesudhas, 1982) (Fig 2 and 3).

In the ascomycete fungi, cells can communicate intercellularly through a cytoplasmic flow that passes through the septal pore (Bloemendal and Kück, 2013). The flow of cytoplasm from older into younger fungal part is essential, as this cytoplasm movement concurrently with organelles migration, such as nuclei and mitochondria. (van Peer et al. 2009). The migration activity has a function to support next-generation life, as well as the new cell that becomes independent to fulfill their energy requirements (Li and Calderone, 2017). During the growth of the younger fungal part, there is communication activity among the cells and organelle (Fischer et al. 2018). This communication becomes critical to recognize the condition of another cell (Bloemendal and Kück, 2013). For example, like a wounded cell that possibly causes cytoplasmic bleeding. WBs will rapidly close the septal pore on the cells that connected with the injured cell (Steinberg et al. 2017b). On another example, there is evidence that nuclei can divide two times to fulfill the requirement of another cell for nucleus presence (Jones et al. 2016).

1.3 Conidiophore structure and organelle migration into conidia

Conidiophores are recognized as aerial or branch hyphae that bear conidia. This fungal structure can be envisaged as the vital bridge that influence organelle during the migration, such as nuclei migration into small conidia (Springer and Yanofsky, 1989; Ishi et al. 2005). In *P. oryzae*, when conidia formation is going to be started, a protuberance arose as a narrow constricted area (Rao and Jesudhas, 1982), cytoplasm and organelle flow that pass through this area will need to adapt to move until reach the conidia area. Study from Jones et al. (2016) showed that nuclei in the invasive hyphae (IH) with ~2 μm diameter can change their surface and form until becoming extremely constricted to enter IH peg with only ~0.5 μm diameter.

1.4 Mitochondrial behavior and fungicide

1.4.1 Mitochondrial behavior in filamentous fungi

Mitochondria are cell batteries that have been recognized for a long time in producing the energy required for cell growth and metabolism. Mitochondria are also organelles always changing their shape and size due to fission and fusion events, called mitochondrial behavior (Westermann and Prokisch, 2002). Currently, their behavior has been known as an essential dynamic that influences many cellular activities to grow young fungal generation (Wai and Langer, 2016; Zhong et al. 2016). Through fission and inheritance behavior, every new healthy cell receives mitochondria from the old cells. Hence, basically mitochondrial morphological changes can regulate physiological activity such as branch hyphae growth (Potapova et al. 2014), or even cell death (Ruf et al. 2018).

Mitochondrial fusion and fission behavior inextricably linked with mitophagy (Ashrafi and Schwarz, 2013). Mitophagy is the process of ingesting damaged mitochondria in autophagosomes which are then degraded to lysosomes. This mechanism cause mitochondria can maintain their quality generally (Sica et al. 2016). Besides, fission behavior can increase the separation of superfluous mitochondria and help their cleansing through mitophagy (Twig et al. 2008; Buhlman et al. 2014). In *P. oryzae*, mitochondrial fission and mitophagy are necessary for invasive infection in rice cells (Kou et al. 2019).

Among the fungal species, mitochondria behavior might be different, because this organelle movement relies on a different system for each species. For example *Neurospora crassa* species has microfilaments and microtubules that involved in positioning and motility of mitochondrial movement. But on another hand, *Aspergillus nidulans* do not require a functional microtubule to migrate its mitochondria

(Westermann and Prokisch, 2002). Hence, study about mitochondria behavior among fungal species will became very interesting and challenging.

1.4.2 Fungal mitochondria as the target of fungicide

As shown previously, mitochondria are critical fungal organelle for supporting cells to live and grow that can be exploited to develop new anti-fungal drugs. Some fungicides have target to disturb electron transport system activity, for example, azoxystrobin (Affourtit et al. 2000). The electron transport system in mitochondria is composed of five complexes, three of which provide mitochondrial ATP (complex I, III and IV) (Figure 5). Therefore, if there is electron transport chain dysfunction, cells will be starved of ATP, cellular synthesis decreases and even triggers cell death (Li and Calderone, 2017).

Mitochondria are highly dynamic organelles; they actively divided (fission) and combined (fusion) in the cell. This activity is necessary for autophagy or mitophagy. Through mitophagy, mitochondria can work efficiently, because only healthy mitochondria that remain in the cells. In *Aspergillus fumigatus* , fusion genes such as Ugo1, Fzo1, and Mgm1 are essential for this fungal viability (Neubauer et al. 2015). If protein produced by this gene is disrupted, then fungi will not grow optimally.

Other targets that can be explored further are protein that supports the mitochondrial activity. Mitochondria are composed of more than 1,000 nuclear-encoded proteins (Calderone et al. 2015). A recent study shows that these proteins have 16 functional categories, where each of the proteins correlates with the mitochondrial organization (Yang et al. 2013). For example, the protein that associates with tricarboxylic cycle (TCA) in the inner membrane, while protein that associates with mitochondrial movement, import, and dynamic located in the outer membrane. If anti-fungal agents inhibit these protein work, then all mitochondrial activity can not become normal.

1.5 Quinol oxidation inhibitors (QoI) and pathogenic fungal resistance

1.5.1 Strobilurin (QoI) as fungicide

Quinol oxidation inhibitors (QoI) are a type of fungicide with a mode of action that inhibits mitochondrial respiration by binding to the Qo site (quinol oxidation site outside) of the cytochrome bc enzyme complex (complex III). The first generation of natural QoI molecules extracted from mushroom *Strobilurus tenacellus* in 1977 was Strobilurin A (Anke et al. 1977). Strobilurin's name is derived from this mushroom name. Strobilurin compounds can easily change with the presence of light (photolabile). With this labile character, it seems difficult to produce strobilurin in mass production. Therefore many industries developed synthetic strobilurin that more stable and robust in agricultural field applications (Balba, 2007), such as azoxystrobin.

Most strobilurin compounds are systemic fungicides that can be absorbed in the leaf tissue, especially in the cuticle (Balba, 2007). Their target is more towards conidia that germinate on the leaf surface rather than mycelium, as fungal conidia are more susceptible to strobilurin compounds than mycelium. Understanding how strobilurin act on the leaf, it will help the farmer to use strobilurin in the rice field effectively. Strobilurin fungicide is more proper to be used as a preventive than curative treatment (Anesiadis et al. 2003). Because after the mycelium can massively invade the plant cell, the use of strobilurin will less useful anymore.

Strobilurin (QoI) quickly becames popular in the market as a powerful fungicide in controlling pathogenic fungi. The sales level can reach over 20% of the global fungicide market within ten year since the first commercial offering (Fernández-Ortuño et al. 2008).

However, after this short market penetration achievement, the incident of some resistant pathogens was reported.

1.5.2 Fungal resistance towards QoI fungicides

The fungal resistance emergence is caused by a mutation in the target site of strobilurin (Qo site). More precisely, mutation located in the mitochondrial cytochrome b gene (*CytB*) causes QoI resistance that prevents fungicide binding. There are two regions of *CytB* that are affected by the mutation and play a role in ligand binding. These domains correspond to amino acid position 120-155 and 255-280 of the encoded protein. Some phytopathogenic fungi that resistant to QoIs have been studied to have amino acid replacements. At position 143 (G143A), glycine is substituted by alanine and at position 129 (F129L), phenylalanine is replaced by leucine (Gisi et al. 2002).

Fungal strains with G143A indicate complete resistance because they always survive and thrive after the QoI application. According to the Fungicide Resistance Action Committee, FRAC, QoI Working Group [www.frac.info] (2012), there are 32 species of phytopathogenic fungal species that have become resistant towards QoI, of which 29 species with G143A. Even though many studies suggested QoI resistance in pathogenic fungi corresponded with G143A substitution, the basic knowledge of the function of amino acid change in fungal resistance has not revealed conclusively. Research about this has been challenging to be conducted as the protein target is encoded in the mitochondrial genomic DNA (Gisi et al. 2002).

A fungal cell may contain mitochondria with one (homoplasmy) or more than one type of mtDNA (heteroplasmy). Some studies mention about fungi with G143A that have mitochondrial heteroplasmy (Lessemann et al. 2007; Vielba-Fernández et al. 2018). This

conclusion can trigger some questions about the evolution of QoI resistance. Until now, how wild-type and mutated mitochondria distributed into a new generation of phytopathogenic fungi and how much mutated-mitochondria required in conidia until fungi become fully resistant towards QoI still unknown.

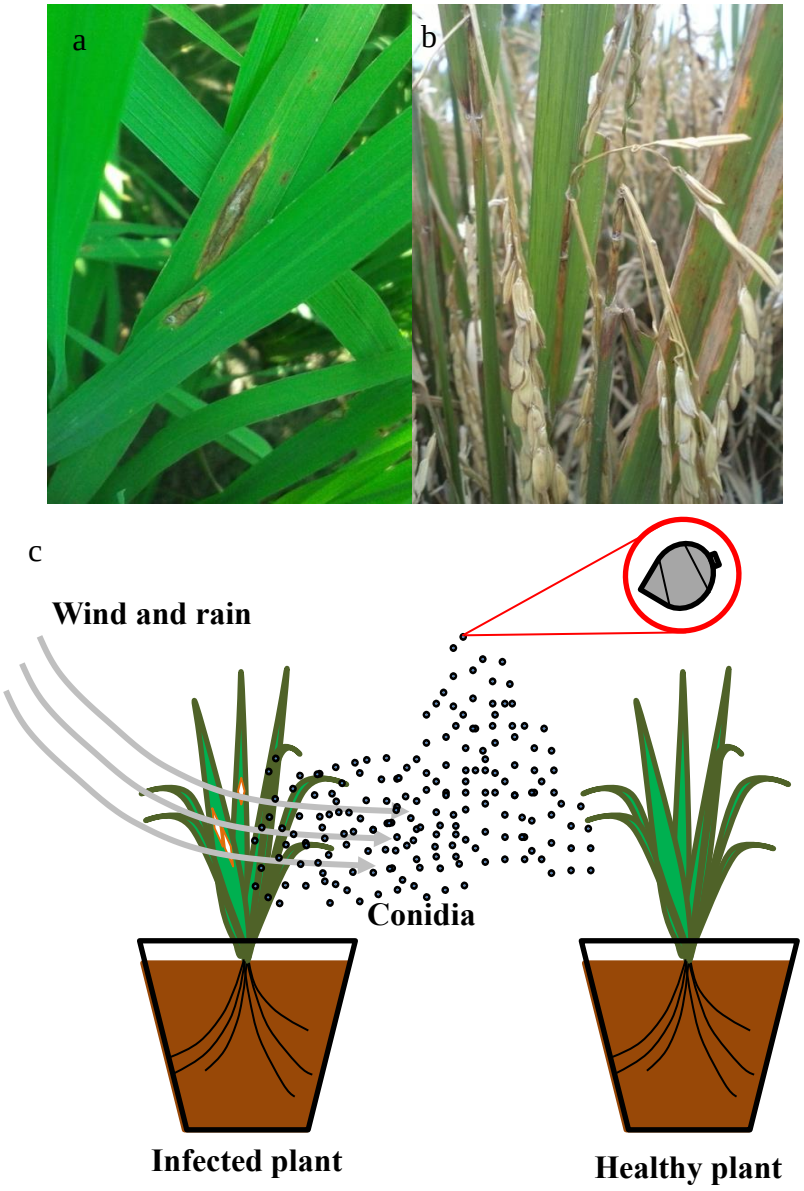


Fig 1.1 The symptom of rice blast fungus and conidial dispersal illustration. (a) spindle shaped of rice blast fungus lesion, (b) fractures in the panicle axis of rice plant after the intensive attack of the disease, (c) conidial dispersal with help from wind and rain from infected to a healthy plant.

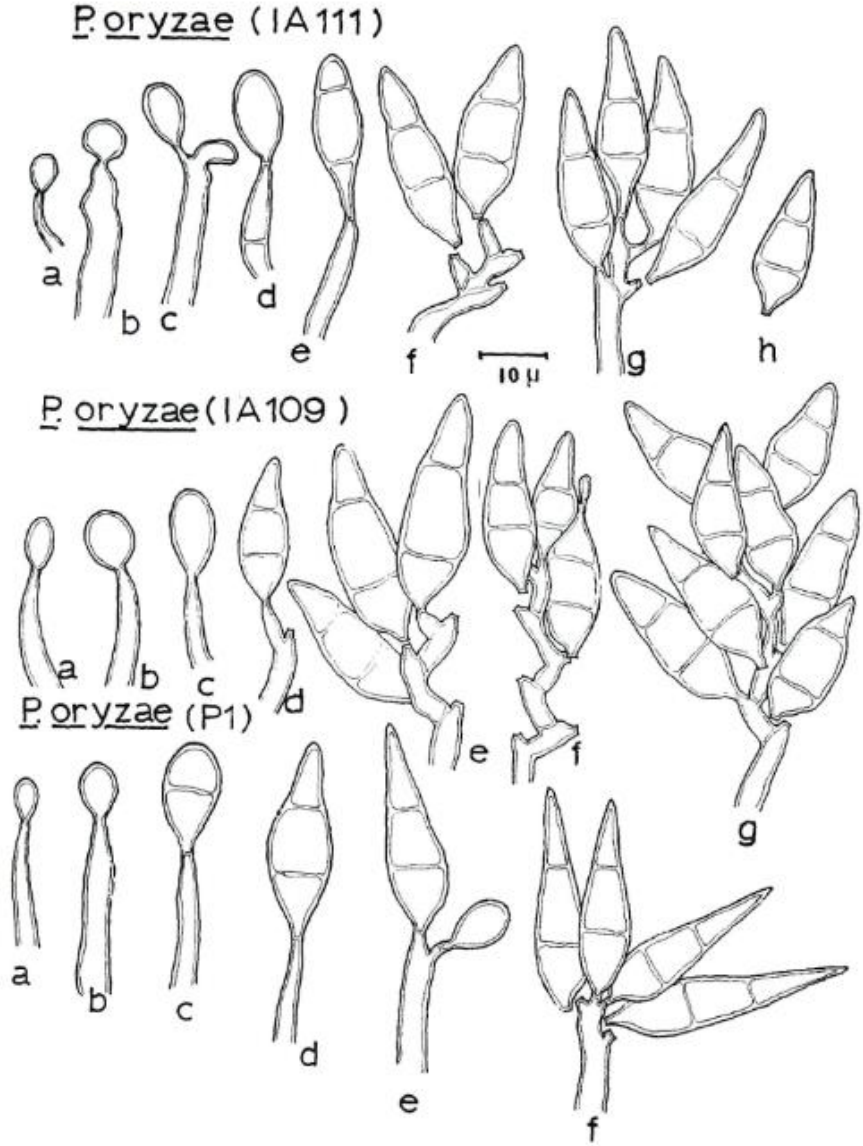


Fig 1.2 Development of conidia in three isolates of *P. oryzae. P. oryzae* (IAlll): (a-e) Development of conidium by simple budding from the tip of the conidiophore. (f-g) Mature, pyriform, 2-septate conidia with geniculate conidiophores. h) Detached conidium with a basal hilum. *P. oryzae* (IA 109): a—d) Stages in the development of conidium. e—g) Geniculation of conidiophores with detached conidia. *P. oryzae* (P 1, wild type): a—b) Development of first conidium initial by budding, c) Two-celled conidium initial with deliminated septum, e) Formation of a second conidium initial with mature conidium on the conidiophore. f) Conidiophore with detached conidia (Rao and Jesudhas, 1982).

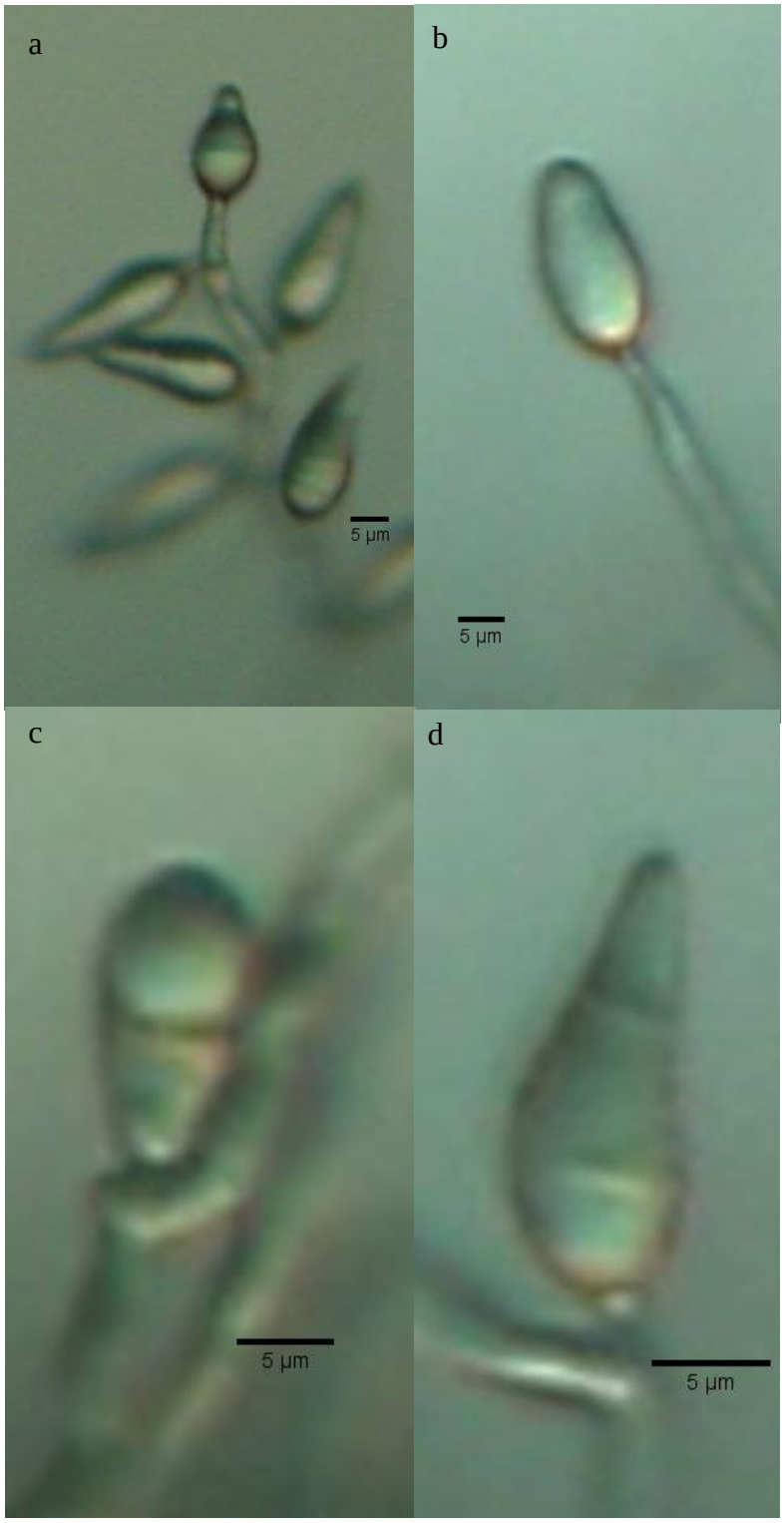


Fig 1.3 Conidia of *P.oryzae*. (a) Conidia development with conidiophore, (b) conidium without septa and conidiophore, (c) conidium with one septum and conidiophore, (d) conidium with two septa and conidiophore.

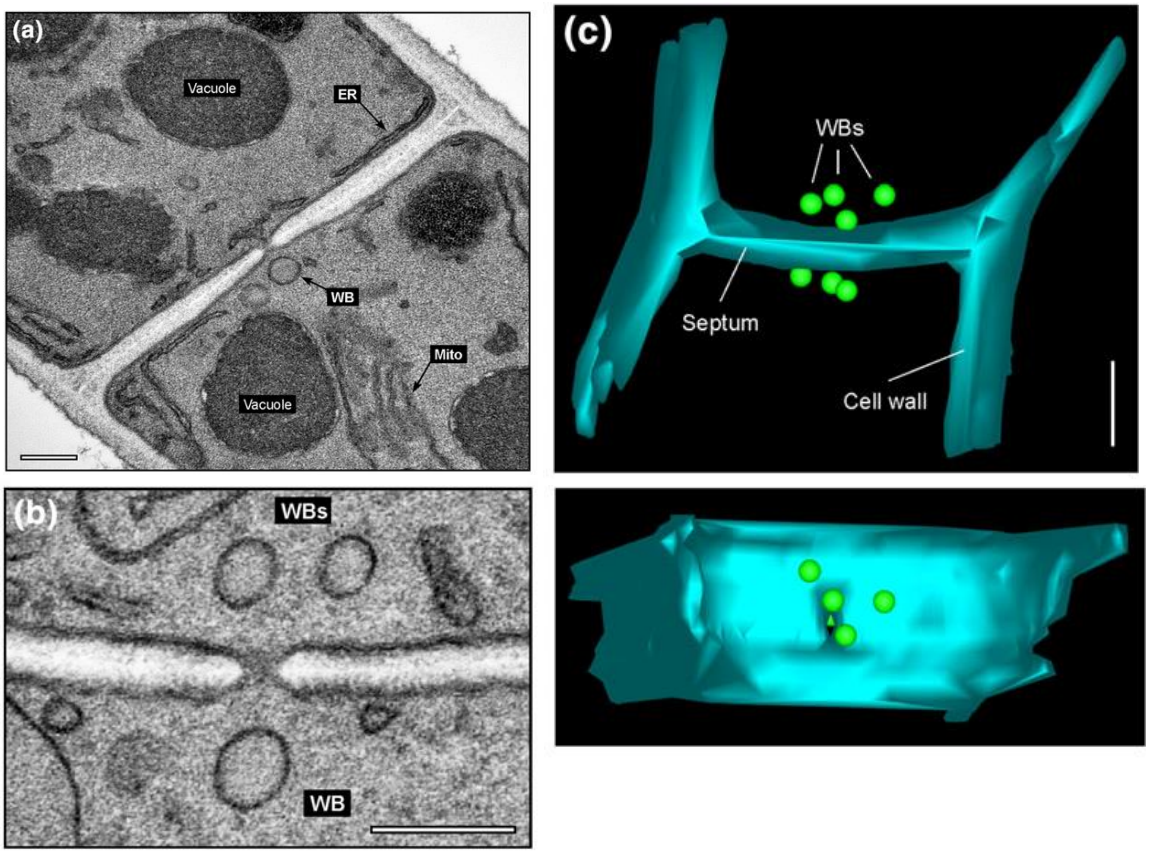


Fig 1.4 Septal pore and woronin bodies in ascomycete fungi, *Zymoseptoria tritici*. (a) Electron micrograph showing a septum in *Z. tritici*. A single Woronin body (WB) is indicated. Scale bar represents 0.2 μm. (b) Electron micrograph showing a septum in Z. tritici. Several WBs surround the septal pore. Scale bar represents 0.2 μm. (c) A 3D reconstruction of serial sections through a septum of *Z. tritici*. Scale bar represents 0.5 μm (Modified from Steinberg et al. 2017b).

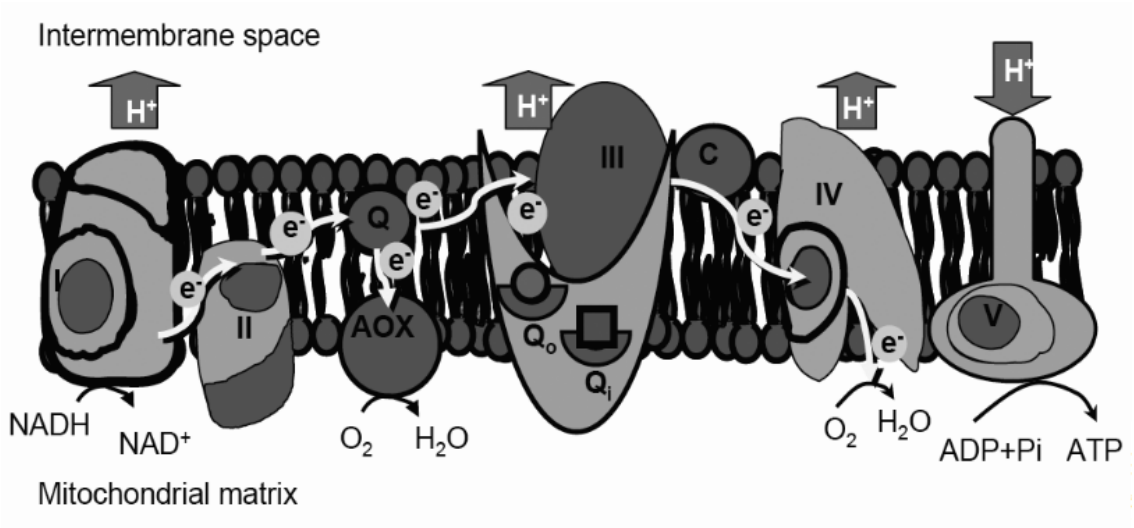


Fig 1.5 Schematic representation of the mitochondrial electron transport system. I, II, III, IV are the different complexes of the transfer chain. V is the ATP synthase complex; Q, the ubiquinone pool; and C, the peripheral protein cytochrome *c*. The arrows inside the membrane indicate the direction of electron flow. Qo and Qi binding sites of the cytochrome *bc* enzyme complex (complex III) are delineated by a circle and a square representing Qo- and Qi-inhibitor molecules, respectively. In some fungi, inhibitors of the respiratory pathway induce the synthesis of alternative oxidase (AOX), which diverts electrons at the ubiquinone pool (Q), although generating much less energy (Fernández-Ortuño et al. 2008).

Chapter 2

Visualizing mitochondria of *Pyricularia* oryzae

2.1 Introduction

Mitochondria are organelles that actively moved, fused, and divided. Within a cell, there might be mitochondria with one or more than one type of mitochondrial DNA (mtDNA). Through random segregation, a fungal cell can have mutated mitochondria that mix with wild-type mitochondria, and it is called heteroplasmy (Wang et al. 2017). Another condition is when a fungal cell has completely one type of wild-type or mutated mitochondria, which is called homoplasmy (Barr et al. 2005). Both conditions raise the question of what happens with both types of mitochondria when they are mixed. Whether mutated or wild-type mitochondria can become dominant or whether mutated and wild-type can be fused to form a second new mutant type.

Fungal cell with mixed mitochondria conditions, which is initially dominated with wild type mitochondria, somehow through segregation might be changed with mutated mitochondria dominance in the new fungal generation. Probably this dominance can cause the fungus to become a mutant. This hypothesis might able to explain how pathogenic fungi can gradually turn into resistant towards QoI fungicide and how the mitochondria are passed on to the younger generation. Their dynamics are remain tried to be explored further, considering the difficulty of observation during the growth and development, especially in the conidia of *P. oryzae*. Then, how we set up an experiment to answer this question becomes an important strategy.

Until now, behavior of mitochondria is still unknown in the fungus *P. oryzae*, especially when they are inherited to conidia. Conidia is the part of the fungus that is most

responsible for the spread of rice blast disease, so knowing how the behavior of the mitochondria in passing down a part of their self to conidia can answer some essential questions. This study can reveal basic knowledge to understand how mutated or wild type mitochondria behave and are inherited. It is even possible in subsequent studies that the behavior of mitochondrial DNA between mutated and wild-type mitochondria can be known, especially when it is inherited and developed in the conidia, starting from baby, young and matured conidia.

Thus, the visualization of mitochondria becomes fundamental in the observation of mitochondrial behavior in the conidia. Genetic transformation can be carried out so that the mitochondria will give the expected color expression under the microscope. There are two types of microscopes used to make these observations, the first is fluorescence microscopy, and the second is confocal laser-scanning microscopy. The first microscope can be used to check whether the transformation has been successfully carried out. While the other microscope can be used to visualize and build 3D images of mitochondria. So that observations will be more thorough in all mitochondrial structures.

Transformation in the fungi can use gene targets in the nucleus that encodes a protein that heading to mitochondria. Most proteins needed by the mitochondria are encoded in the nucleus and synthesized at the cytoplasmic ribosome cytosol, which is then sent to the mitochondrial inner membrane. In this transformation of *P. oryzae* has been carried out by utilizing citrate synthase (CitA)-green fluorescent protein (GFP) fusion. Citrate synthase is a protein encoded from the nucleus of the cell, which then moves to the mitochondria to meet the protein requirements in the tricarboxylic acid cycle (TAC). By attaching GFP to CitA, this GFP will make mitochondria to express green color under a

fluorescence microscope. Through 3-dimensional visualization of mitochondria in the conidia, analysis can be done to reveal mitochondrial distribution patterns.

2.2 Materials and Methods

2.2.1 Fungal culture and filter paper stock preparation

Citrate synthase (CitA)-Green Fluorescent Protein (GFP) fusion was utilized to visualize mitochondria in *P. oryzae*, according to the report by Suelmann and Fischer (2000) on *Aspergillus nidulans*. Briefly, DNA sequence encoding N-terminal part of CitA (Accession: MGG_07202) was PCR-amplified with two primers (5´-ATGGCCTCTGCTATGCGC-3´ and 5´-CTGGTCAAGAGTGACCTTGTC-3´) and cloned into the N-terminal of EGFP gene in pBLASTR-TEF1::eGFP::Mop53BP1 (Ohara et al. 2018) using NEBuilder HiFi DNA Assembly Master Mix (New England Biolabs Japan, Tokyo, Japan). The vector was then inverse-PCR amplified with two primers (5´-GCGACGGCCCCGTG-3´ and TAGGGGATATCAGCTGGATGG-3´) and re-circularized to get rid of Mop53BP1 gene and introduce a stop codon for EGFP. The resulted vector, pBLASTR-TEF1::CitA::eGFP was used for the transformation of *P. oryzae* Ina86-137 strain according to the method by Miki et al. (2009). The transformation was confirmed with PCR and Southern hybridization of *CitA*-EGFP fusion gene.

Pyricularia oryzae INA 86-137 (Cit-GFP) was cultured on the oatmeal agar and prune agar with incubation time for two weeks with temperature 25 °C under fluorescence light. The filter stock was prepared with culturing the fungus on the prune agar covered with filter paper pieces (5 mm^2). After the fungus covered the surface, the filter paper pieces were transferred into vials and dried up using a desiccator for two weeks. The filter

paper was stored in the freezer at -20°C. This filter paper stock could be used to reculture INA 86-137 (CitA-GFP).

2.2.2 Washed treatment and cut agar

INA 86-137 (CitA-GFP) was cultured for two weeks. After that, all colonies on the agar were washed and discarded with sterilized distilled water (SDW) until seven times. Each washing time, it was used 10 ml of SDW to eliminate the fungal colony. Petri dish with washed agar medium was air-dried in the laminar airflow for about 10 minutes. The agar medium was cut with a size 1 cm x 1 cm and was placed into a small Petri dish. Agar pieces were incubated under fluorescence light with 25 °C for 30, 33, 36, and 72 hours. For each incubation time, three Petri dishes as replicates.

2.2.3 Conidia concentration

Conidia were harvested using SDW, scraped by cell scraper, and conidia suspension were sieved by Miracloth (Calbiochem) and placed into 50 ml tubes. From 50 ml tubes, conidia suspension was concentrated using microtubes 1.5 ml and refrigerated centrifuge 15,000 rpm 4 °C until becoming 10 or 20 µl. Conidia with one, two, and three cells number were counted with a hemocytometer and were calculated to know conidia concentration each ml.

2.2.4 Conidia Fixation, Mitochondria, and fungal wall Staining

Conidia were fixed with formalin 5% for 10 minutes before observation. To comparison with CitA-GFP transformation, conidia were stained with MitoTracker Red CMXRos 300 nM in 37^0C for 30 minutes. To ensure how many cells in the conidia during further observation, calcofluor white (CFW) was used to stain the conidia wall with a blue color.

2.2.4 Observation and acquisition 3D images of mitochondria

Observation of mitochondria was conducted with fluorescence microscopy BX50 (Olympus) for comparing the result from (CitA)-GFP and MitoTracker. 3D images of mitochondria were acquired by Confocal microscopy Leica TCS SP8 STED 3X and Las X software using HC PL APO CS2 100x/1.40 (Oil), equipped with laser Diode 405 and WLL (70%). Conidia were exposed by laser with excitation/emission wavelengths were 488 nm/498– 530 nm (CitA-GFP) and 405 nm/520-530 nm (Calcofluor White).

2.2.5 Analysis of 3D visualization of conidial mitochondria

Analysis of the relationship between conidial cell number and categorization of conidial mitochondria was analyzed by the enumeration of conidia with each category of mitochondria. Seventy-five conidia of each number of the cell were selected to build 3 dimensional-object of mitochondria. Within each cell number, conidia were grouped into based on mitochondrial morphology appearance, such as dot when mitochondria appearance was only dotted and as tubule or network when we could find tubule or network form in the conidia cell.

2.3 Result

2.3.1 The use of calcofluor white for staining conidial wall

The results showed that calcofluor white (CFW) can color the walls of conidia. With its blue expression, the number of cells in the conidia can be distinguished very clearly and more easily. Besides, the CFW image can be merged with the CitA-GFP image, this result indicates that CFW compatible with (CitA)-GFP (Fig 2.1).

2.3.2 The use of MitoTracker to confirm (CitA)-GFP for staining mitochondria

The results showed that both green colors from (CitA)-GFP and red color from MitoTracker colocalized inside conidia (Fig. 2.2). Both colors indicate almost at the same

position after merged. Based on this result, it suggested that (CitA)-GFP is a reliable method to visualize mitochondria in the *P. oryzae*.

2.3.3 Identification of the appropriate timing condition

The result shows that there are no conidia found at 30 h, while after 33 h, conidia with one, two, and three cells were harvested. Interestingly, the percentage of conidia with one cell and two cells decreased as the time of incubation increased, but remains at 5.3% and 16.4%, respectively even after 72 hours (Fig. 2.3a). These results indicated that the conidia development in this transformant starts after 30 h of incubation, and at least a part of single cellular conidia in 33 to 36 h incubation will be developed to three-cells conidia in 72 h. In addition, microscopic observation of conidiophore showed the formation of conidia in 36 h of incubation (Fig. 2.3bc). Based on these results, the appropriate time point for the observation of a variety of conidia was confirmed as 36 h incubation. Conidia with one cell, two cells and three cells harvested at 36 h incubation were indicated in Fig.2.4.

2.3.4 Analysis of Conidial mitochondrial 3D visualization

Through 3D visualization, we would able to observe the display of the mitochondria from many angles so that we could understand the mitochondrial structure much better rather than 2D visualization. In conidia, mitochondria were observed based on various 3D morphology and the length, mitochondria were categorized into dots, tubules and networks (Table 1 and Fig 2.6a-c). The relationship between conidial cell number and categorization of conidial mitochondria was analyzed by the enumeration of conidia with each category of mitochondria. 75 conidia of each number of the cell were selected to build 3 dimensional-object of mitochondria. Within each cell number, conidia were

grouped into based on mitochondrial morphology appearance, such as dot when mitochondria appearance was only dotted (Fig. 2.6d) and as tubule or network (Fig 2.6e-f) when we could find tubule or network form in the conidia cell (Fig. 2.5). All types of conidia were dominated by network mitochondria (Fig. 2.5). There are a few single cellular conidia that could be found without mitochondria and contained with only dot mitochondria.

In addition, mitochondria in hyphae were observed with the same method (Fig 2.6g-l). The appearance of mitochondria in hyphal tips was observed mainly as dots, and those in the basal part of hyphae were mainly as tubules (Fig. 2.6g-i). In Fig. 2.6j-l, the morphology of mitochondria was compared in the branch and main hyphae, which is considered as young and matured hyphae, respectively. These results showed that mitochondria in the primary hyphae formed as a network, while in the branch, hyphae formed more dominant with dots and tubules.

These results might suggest that mitochondria are distributed to conidia as a dot because hyphal tips with dot mitochondria are considered as conidiation parts as observed in Fig. 2.4d. In addition, only a few single cellular conidia had only dot type mitochondria. However, on the other hand, single cellular conidia with network-type mitochondria were also found in 36 h of incubation. Based on the fact that single cellular conidia could be harvested in 72 h of inoculation (Fig 2.3), it is suggested that some part of conidia could be matured without further division of the cell. The network-type mitochondria in single cellular conidia in 36 h might be matured already. This should be verified by further direct observation of conidia development.

2.4 Discussion

MitoTracker has been developed especially for staining mitochondria (Zhang et al. 2015) and Calcofluor white is used for staining fungal cell walls (Wang et al. 2018). Both of them have been conducted in *P. oryzae* research previously. Besides, in another research, through staining mitochondria using MitoTracker in *Neurospora crassa*, the mitochondrial organization in growing hyphae could be observed and with additional CFW septa in the hyphae could be indicated under the microscope (Potapova et al. 2011; Potapova et al. 2014).

A study from Li et al. (2018) explained that transformation in *P. oryzae* could produce incomplete septa and lacked of any septum. It seems that it will be related to MoCDC14. MoCDC14 is important gene in the fungal species for septation and also virulence of *P. oryzae* (Li et al. 2018).

Some mutants of *P. oryzae* had been known for different abilities and timing to produce conidia (Han et al. 2018; Goh et al. 2017). Conidia production ability is concerned with mitochondrial behavior. The evidence from another study suggested that mitochondrial fission protein MoFis1 mediates conidiation (Zhong et al. 2016) shows the relationship between mitochondria fission and conidiation by the regulation of mitophagy, which is essential for the formation of dot mitochondrion. In *Saccharomyces cerevisiae*, however, the initial form of mitochondria that are distributed to daughter cells as tubule mitochondria (Osman et al. 2015).

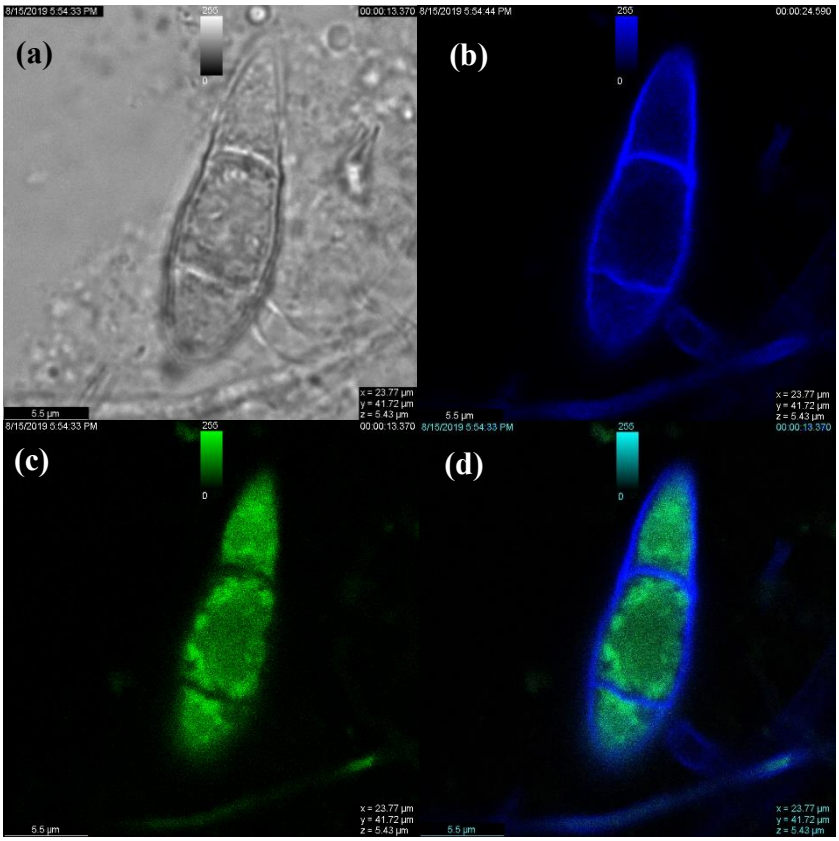


Fig 2.1 Conidia of *P. oryzae*. Conidia in the bright field (a), Conidia with calcofluor white (b); CitA-GFP (c), merged images between calcofluor white and CitA-GFP (d).

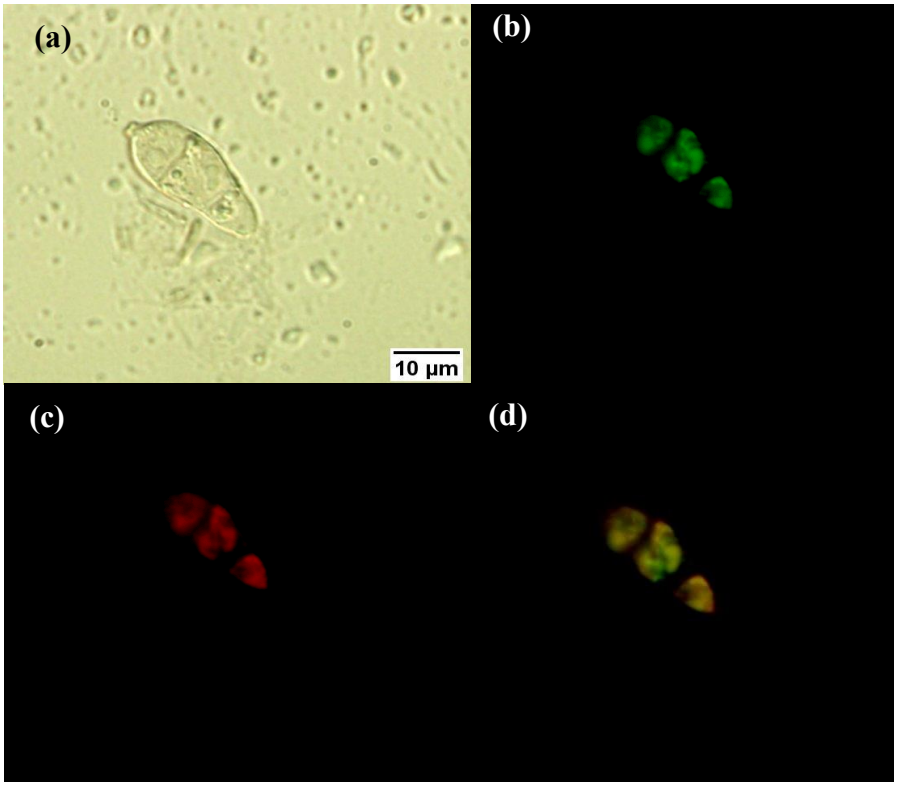


Fig 2.2 Conidia with 3 cells and mitochondrial appearance. Mitochondria appearance under fluorescence microscopy with bright field (a), citA-GFP (b), MitoTracker (c) the merged image between the result from citA-GFP (green) and MitoTracker (red) (d). The observation was conducted by using fluorescence microscopy BX 50 and the pictures were adjusted with ImageJ Fiji (https://imagej.net/Fiji) for the contrast and brightness.

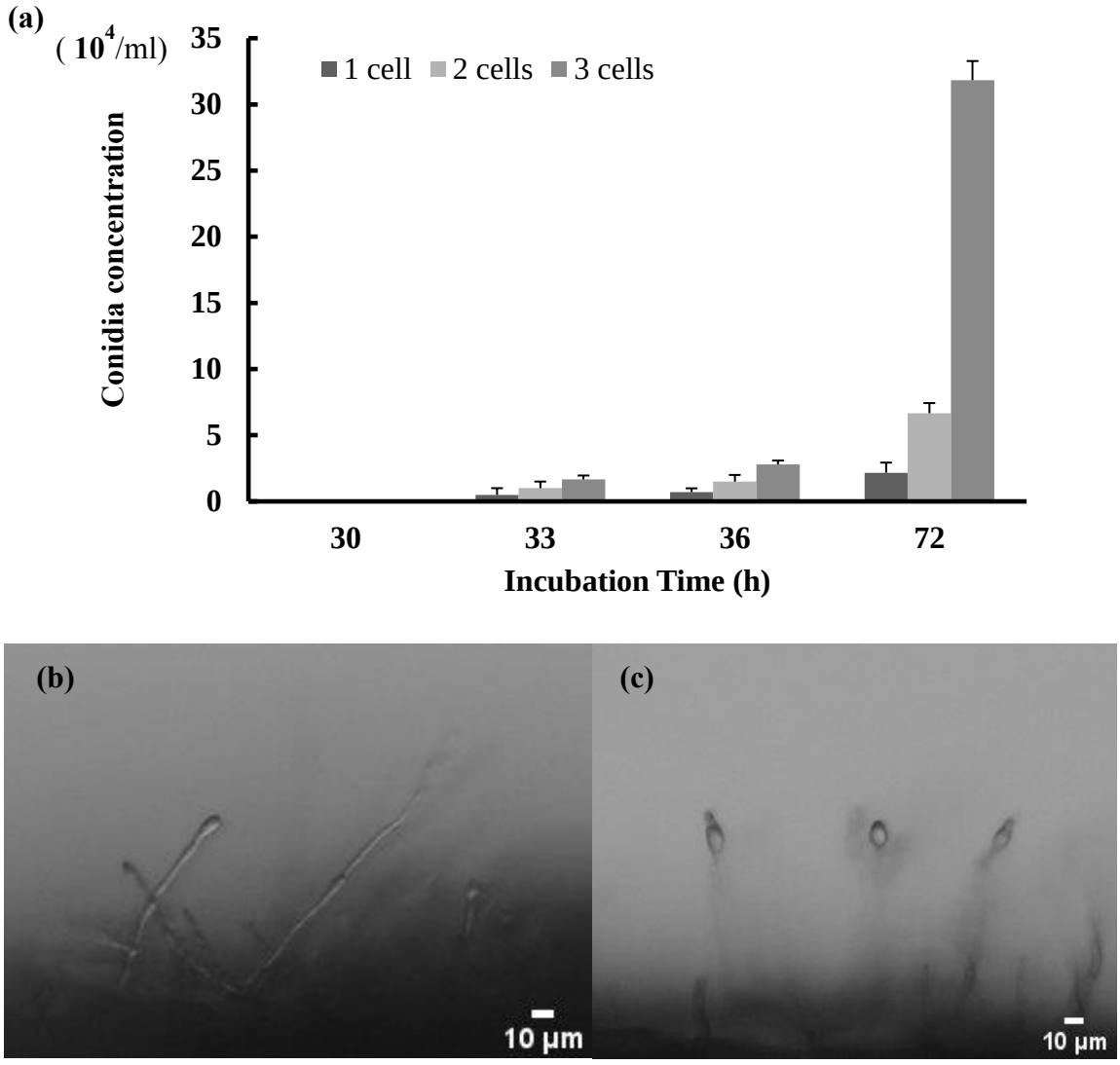


Fig 2.3 Identification of the appropriate timing to observe conidiation. Conidia concentration after 30, 33, 36 and 72 h (a). The bar scale in the graphic indicate standard deviation with 3 replicates. The appearance of conidiophores after 30 h (b) and 36h (c) on slide culture.

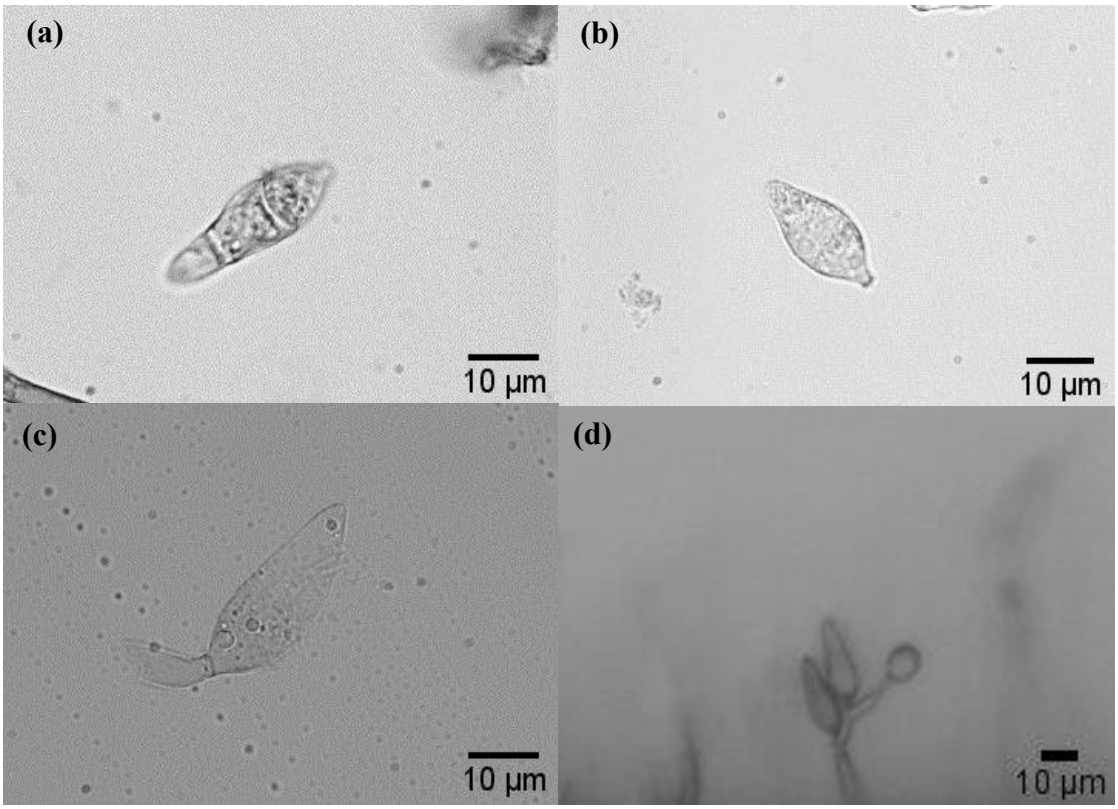


Fig 2.4 Conidia with different number of cells. Microscopic image of conidia with 3 cells (a), 2 cells (b), 1 cell (b) and intact conidia with conidiophore (d)

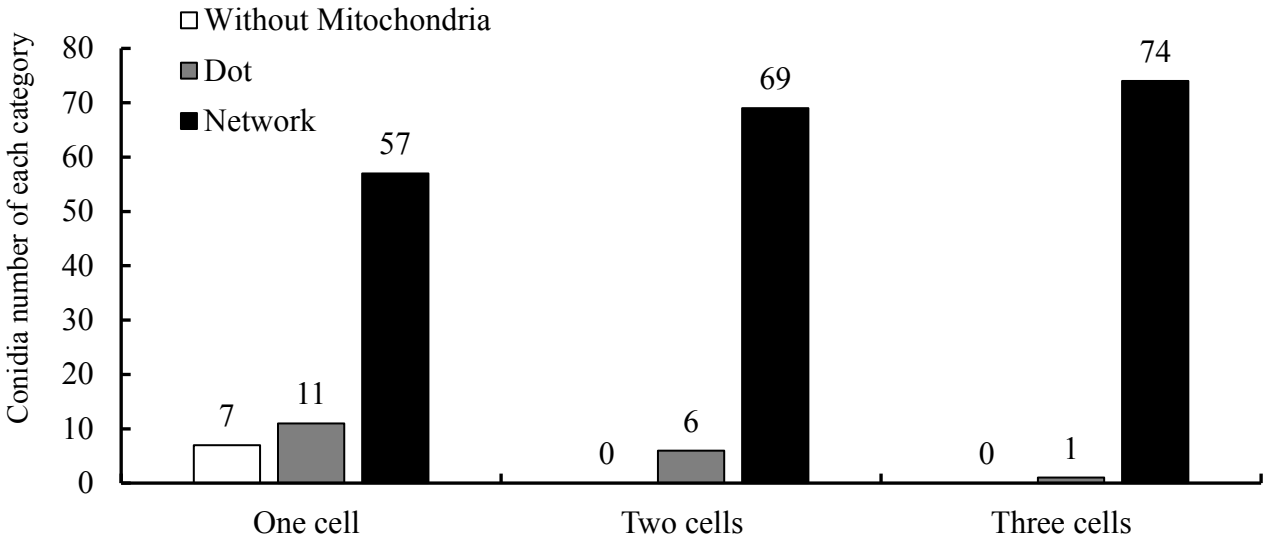


Fig. 2.5 Mitochondria morphology in each type of conidia. Conidia were categorized based on their cell number. 75 conidia were selected to build 3 dimensional-object of mitochondria. Within categories, conidia were grouped into based on mitochondrial morphology appearance, such as dot when mitochondria appearance was only dotted and as tubule or network when we could find tubule or network form in the conidia cell. For example, a conidia with all types of mitochondria was categorized as network. No conidia was categorized as tubule, which contains only tubule or mixture of dot and tubule.

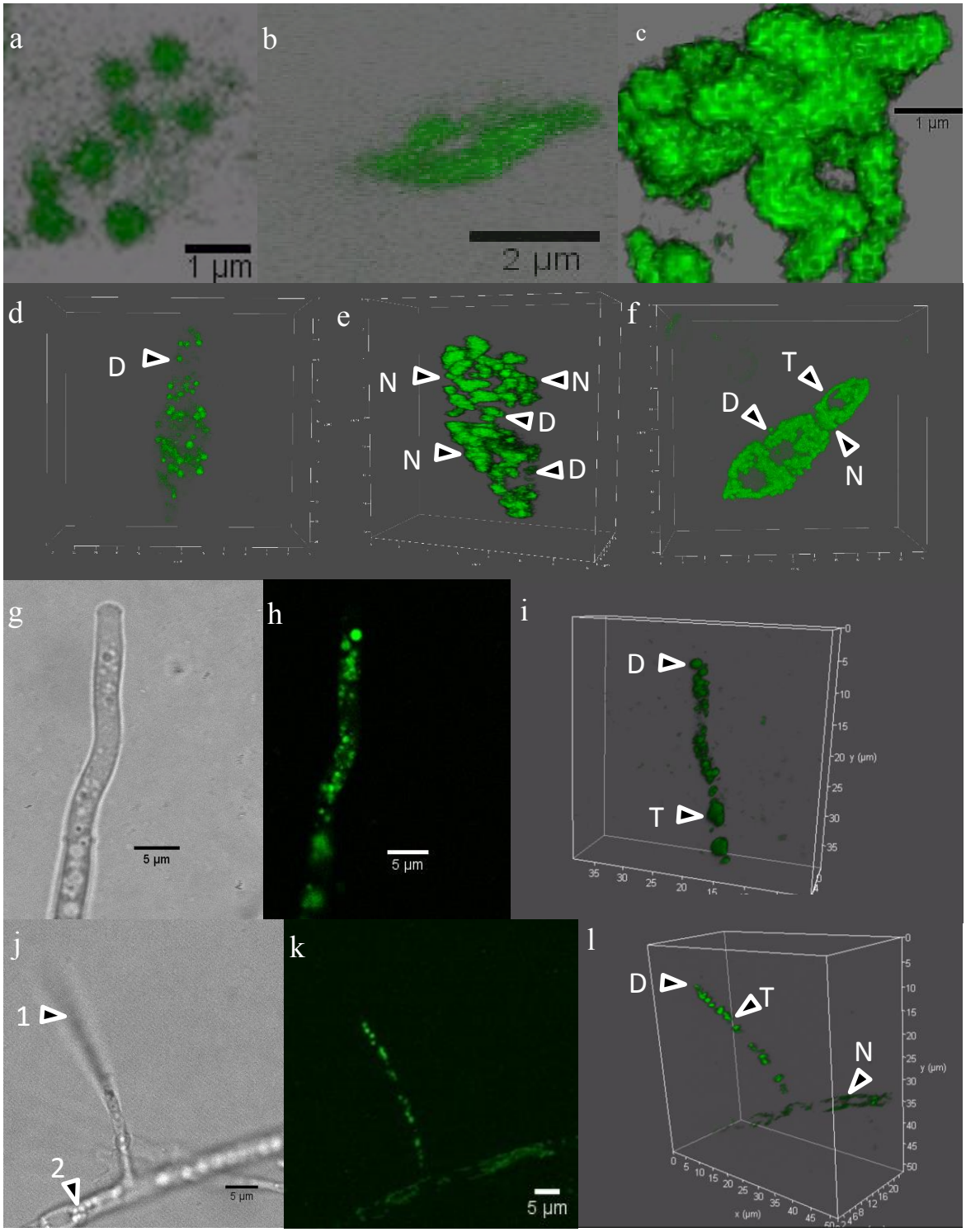

a
1 µm
b
2 µm
c
1 µm
d
D
e
N
N
D
N
D
f
T
D
N
g
5 µm
h
5 µm
i
D
T
y (µm)
j
1
2
5 µm
k
5 µm
l
D
T
N
y (µm)
x (µm)

Fig 2.6 Mitochondria morphology in the conidia and hyphae. Typical 3D image of mitochondria as dots (a), tubules (b), network (c). 3D image of mitochondria in the single-cellular (d), two-cellular (e) and three-cellular conidia (f). Bright field image of hyphae (g and j). Confocal image and 3D image of mitochondria in the hyphal tips (g, h, i, j, k and l). D, N and T arrowheads indicate dot, tubule and network mitochondria, respectively. 1 and 2 arrowheads indicate the hyphal branch and main mycelia, respectively.

Table 1. Category of Mitochondrial morphology of *P. oryzae*

Category	**Description**	**Length (μm)**
Dots	Circle and like ball	0.23-0.75
Tubules	More oval, not branched and formed like a tube	> 1.6
Network	Tubules branched and connected	> 1.6

Chapter 3

Quantification of Conidial Mitochondrial Volume using MitoGraph software

3.1 Introduction

The distribution pattern of mitochondria in the conidia of *Pyricularia oryzae* until now still unclear. In order to analyze their dynamics, it is vital to determine its quantification method. The quantitative value of the mitochondria could be used for further statistical analysis. So, the conclusions from the study of mitochondrial behavior can be more accurate. The previous study attempts to analyze the morphometric image of mitochondria using ImageJ or Image-Pro Plus 5.1 (Media Cybernetics) to analyze quantification of mitochondrial aspect ratio, form factor and number of mitochondria per cell (Koopman et al. 2006; Cribbs and Strack, 2009). In many research studies, observation of mitochondria dynamics was conducted with 2D analysis, while recently study from Nikolaisen et al. (2014) suggested that 3D analysis is the more preferred method, especially when fragmentation happened in the mitochondria, the result showed more detail data to explain this phenomenon.

Mitochondrial quantification is a challenging study, as mitochondria are highly active organelle with diverse shapes from round until becoming interconnected web. Therefore, quantification based on 3D analysis will give more information about the mitochondrial structure and behavior. MitoGraph is an open-source software that can quantify mitochondrial volume in the living cell organism (Viana et al. 2015). This software has been tested using *Saccharomyces cerevisiae* to measure mitochondrial volume (Rafelski et al. 2012). Another research from Harwig et al. (2018) also used

MitoGraph software to measure the mitochondrial amount in the mammalian cell. Hence, this study is the first research that uses MitoGraph in the filamentous fungi, *P. oryzae*.

Generally, conidia will develop from one cell until becoming three cells; however, after transformation, even though most of them grow until becoming three cells, some conidia remain in the same condition as conidia with one cell or two cells (Li et al. 2018). Nevertheless, quantification towards conidia with one, two, and three cells is essential to reveal basic information about mitochondrial amount distribution and make an analysis based on it. This observation has a purpose to know mitochondrial development patterns through their amount changes.

3.2 Materials and Methods

3.2.1 Fungal culture and conidia preparation

Pyricularia oryzae strain INA 86-137 (CitA)-GFP was cultured on the oatmeal agar and incubated under fluorescence light with temperature 25°C for two weeks. After that, all colonies from the agar surface were washed and eliminated. Then, the cultures were incubated for 36 h under fluorescence light. Conidia were harvested and fixed with formalin 5%.

3.2.3 Slide glass preparation

Conidia suspension concentration was taken 3 µl by micropipette and dropped on a slide glass. Conidia suspension on slide glass was given a cover glass. The cover glass was sealed by nail polish with a clear color. This nail polish kept the water under cover glass not to evaporate.

3.2.4 Z stack images acquisition and confocal microscopy set up

Z stack images were acquired by Confocal microscopy Leica TCS SP8 STED 3X and Las X software using HC PL APO CS2 100x/1.40 (Oil), equipped with laser WLL

(70%). Conidia were exposed by laser with excitation/emission wavelengths were 488 nm/498– 530 nm (CitA-GFP). Z stack images were set up with 1024 x 1024 resolution, with z step size 0.2 µm.

3.2.5 MitoGraph and Technical Procedure

MitoGraph software V3.0 could be downloaded from http://rafelski.com/susanne/MitoGraph or https://github.com/vianamp/MitoGraph. MitoGraph was operated under mac Operating System. After downloading, there were five files that we could obtain, (1) CropCells.ijm; (2) GenFramesMaxProjs.ijm; (3) LICENSE; (4) MitoGraph; (5) README.md. File (1) and (2) were macros that could be opened in ImageJ software (https://imagej.net/Fiji) (Figure 3.3), these two macros had a function to prepare MitoGraph input files. After the input files were ready, MitoGraph Software could be operated from a terminal in the iMac or Macbook. In this study, MitoGraph was operated with iMac (21.5-inch, Late 2013) macOS High Sierra, Processor 3.1GHz Intel Core i7, Memory 16 GB 1600 MHz DDR3, Graphics NVIDIA GeForce GT 750M 1024 MB, Series Number C02M70D3F8J8. MitoGraph output (VTK files) could be opened by Paraview software (Fig 3.2).

MitoGraph could be saved in the desktop of the computer, so that the operational analysis using this software would become easier. To prepare MitoGraph input files, steps below could be done (Fig 3.4):

1. A folder named Data was created to save 3D z-stack image of conidial mitochondria
2. Macro “GenerateFramesMaxProjs.ijm” was run with imageJ to generate 3D z-stack image in the Data folder. Then, a new file named MaxProjs.tif would be created and saved in the same folder.

3. MaxProjs.tiff was opened in the imageJ. Region of interest (ROI) was made to indicate mitochondria. the brightness and contrast of MaxProjs.tiff was adjusted with imageJ to help draw ROI . Then, ROI was saved as RoiSet.Zip in the Data folder. “t” was pressed to open ROI manager in the imageJ, “show all” and “labels” were selected to keep track of all the marked cells.
4. Macro “CropCells.ijm” was run in the imageJ with target RoiSet.Zip in the Data folder. This macro took the region bounded by ROI in all frames of MaxProjs.tiff and paste them into a new file named cell. Files in the cell folder were MitoGraph input.

3.2.6 Statistical analysis

Statistical analysis and graphics were made by Microsoft office excel 2016. To understand mitochondrial amount changes, mitochondrial volume was analyzed with regression and correlation method against conidial length. Distribution mitochondrial volume for conidia with different cell numbers was indicated in different colors.

3.3 Result and Discussion

3.3.1 Modification of macro CropCells.ijm

MitoGraph is designed to generate the mitochondrial volume of *Saccharomyces cerevisiae,* hence the resolution is designed only for 200 x 200. In this study, conidial mitochondria are saved with high-resolution 1024 x 1024. Therefore, to process this file, macro CropCells.ijm need to be modified. Modification in the macro CropCells.ijm as follow:

1. **Original script:** // Defining the size in pixels of the single cell z-stacks

_xy = getNumber("Single cell image size in pixels", 200);

Modified script: // Defining the size in pixels of the single cell z-stacks

_xy = getNumber("Single cell image size in pixels", 1024);

2. **Original script :** run("Make Band...", "band=5");

Modified script : // run("Make Band...", "band=5");

3. **Original script** : // run("Add Specified Noise...", "slice standard=" + 0.5*std);

Modified script : // run("Add Specified Noise...", "slice standard=" + 0.5*std);

3.3.2 Run Mitograph

MitoGraph software is run in the iMac terminal. To open the software, change the directory to the location of MitoGraph (cd ~/Desktop/MitoGraph) (Fig.3.2). MitoGraph can be run with the following command line using modified default setting (./MitoGraph -xy 0.024 -z 0.2 -rad 0.15 -scales 2.7 4.8. 45 -adaptive 2 -path ~/Desktop/Data3/cells19). Where the flag -xy 0.024 refers to the xy pixel size in μm (xy depend on each image size condition); -z 0.2 refers to z spacing also in μm; -rad 0.15 refers to tubules radius (default); -scale 2.7 4.8 45 refers to scale range to adjust the picture (default 1.0 1.5 6); -adaptive 2 can make MitoGraph to the image split into 2 x 2 blocks before the segmentation. Scale and adaptive can played to adjust the 3D image until becoming an optimum shape. The sample of Mitograph output can be seen in Fig 3.5. With high-resolution 1024 x 1024, each file required about 45 minutes to be analyzed. It seems that using lower resolution such 256x256 can be a better solution to get faster results. Besides, manage files with low resolution is much easier than the high-resolution image.

3.3.3 Mitochondrial volume against the conidial length

There are two different ways to calculate mitochondrial volume in the MitoGraph software. First, volume based on the number of the voxel (3D pixel) contained within the bounds of this surface represents the surface volume. Second volume based on length of

the 3D skeleton of the mitochondrial network and calculate the skeleton-based mitochondrial volume by assuming that the mitochondrial are tubules with constant radius (150 nm) (Viana, 2015) (Fig 3.5).

Thus, regression and correlation analysis showed that mitochondrial volume based on voxel (surface) or length (skeleton) was not demonstrated a significant difference against conidial length (Fig 3.6 and Fig 3.7). This result was different from the result of Rafelski et al. (2012), they showed that mitochondrial volume increased with the increase of yeast size. Based on mitochondrial distribution analysis from one cell until three cells, some of the conidia increased the mitochondrial volume (Fig 3.8 and Fig 3.9). This result showed that conidial growth was not synchronized with mitochondrial development. Therefore observation and quantification of mitochondrial volume during conidia development become essential so that we can see the more complete story of mitochondrial dynamic in conidia of *P. oryzae*.

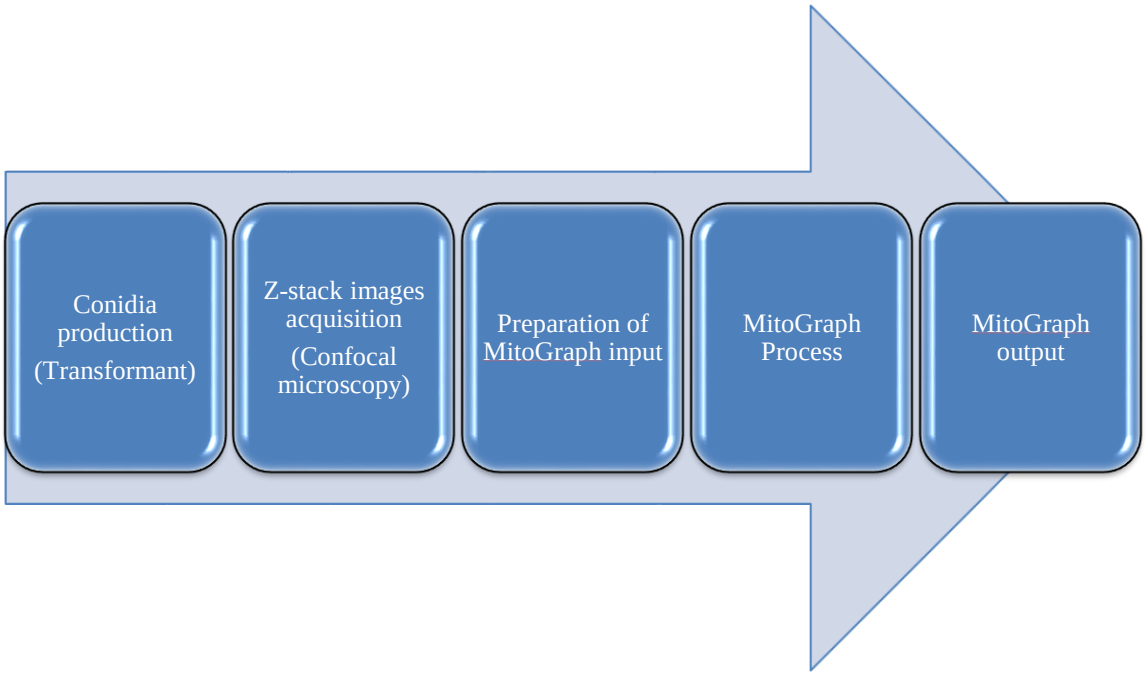


Figure 3.1 The workflow of the study of conidial mitochondrial volume measurement

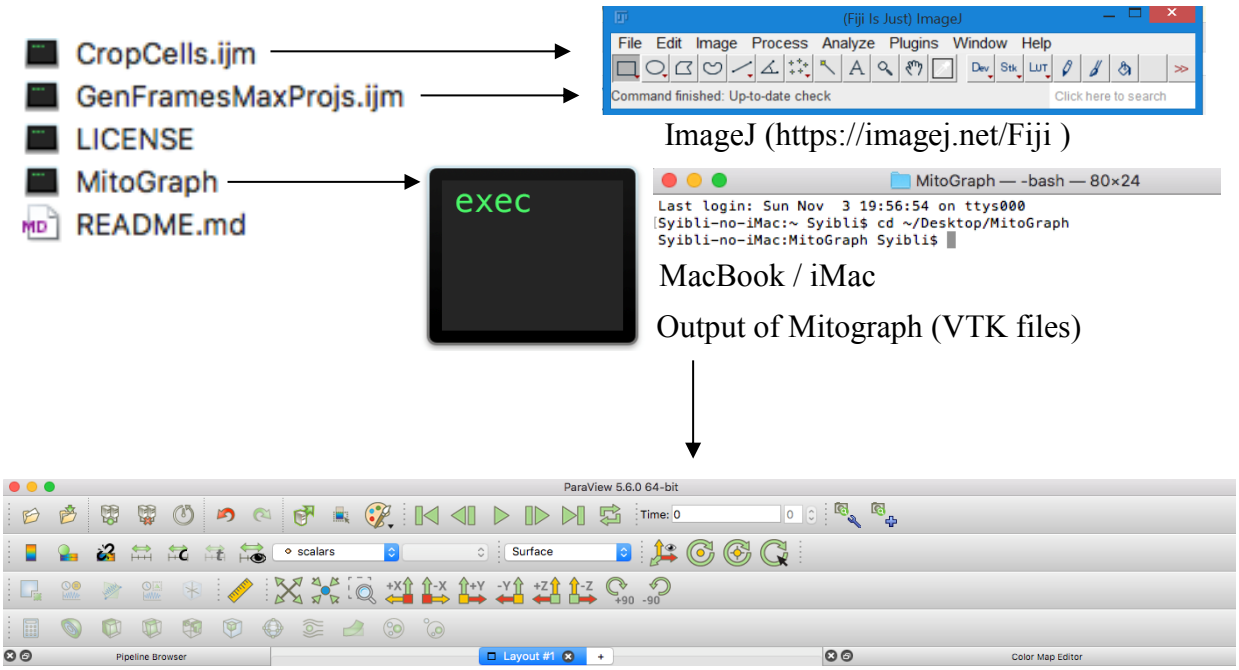


Fig. 3.2 MitoGraph Software and the supporting software. MitoGraph, ImageJ, iMac terminal, and Paraview Software. Arrow showed that the files could be opened by the indicated software

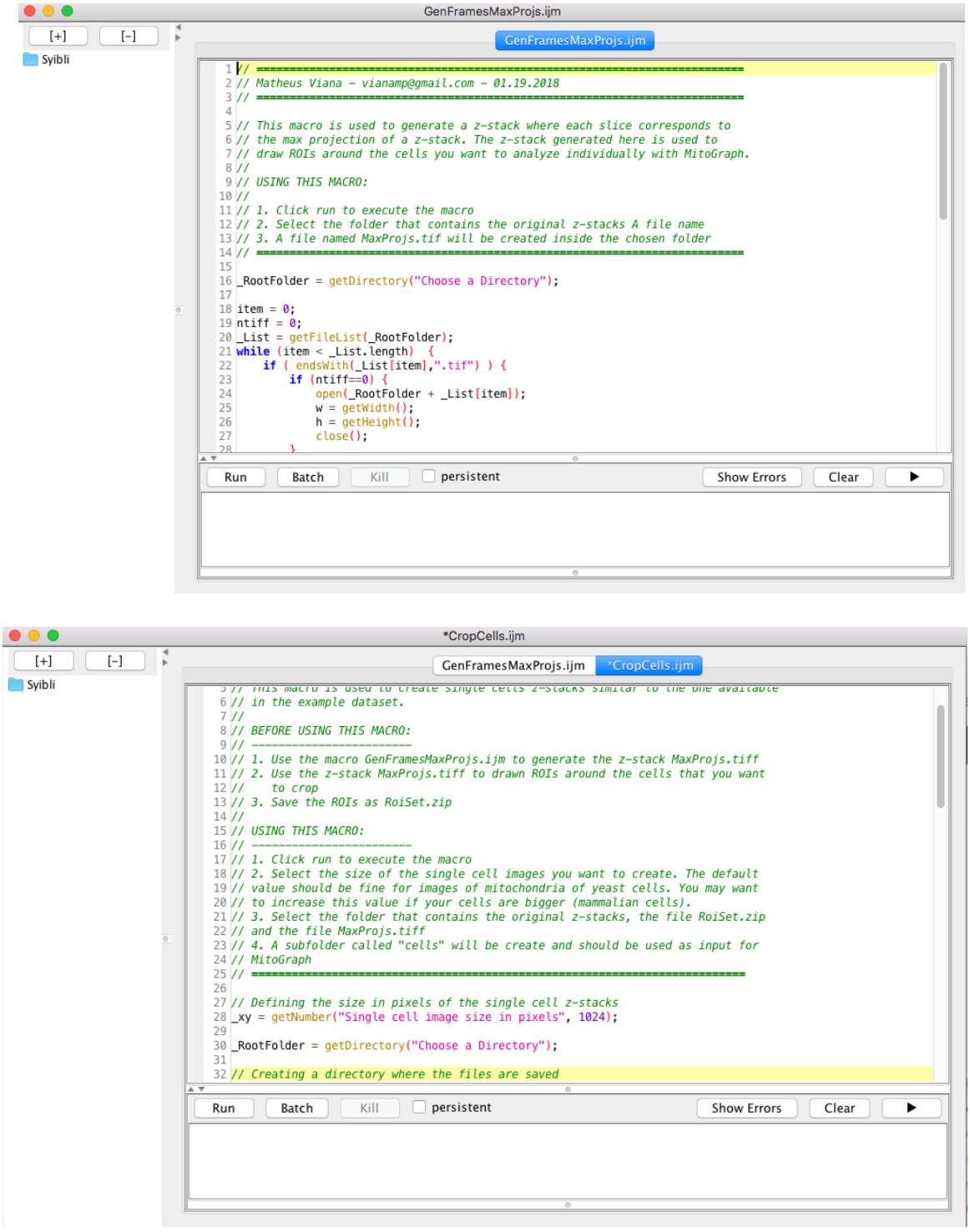
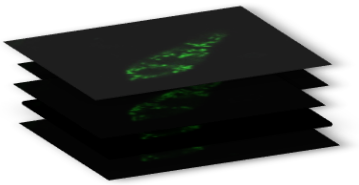
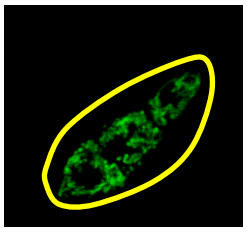


Figure 3.3 The display of GenerateFramesMaxProjs.ijm and CropCell.ijm



Z-stack images. tif

1. Z-stack images were processed by ImageJ Fiji software https://imagej.net/Fiji



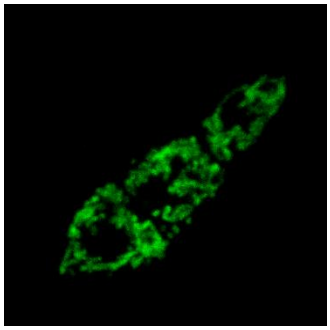
MaxProjs.tif

2. Run GenerateFramesMaxProjs.ijm +ROI Drawing with ImageJ



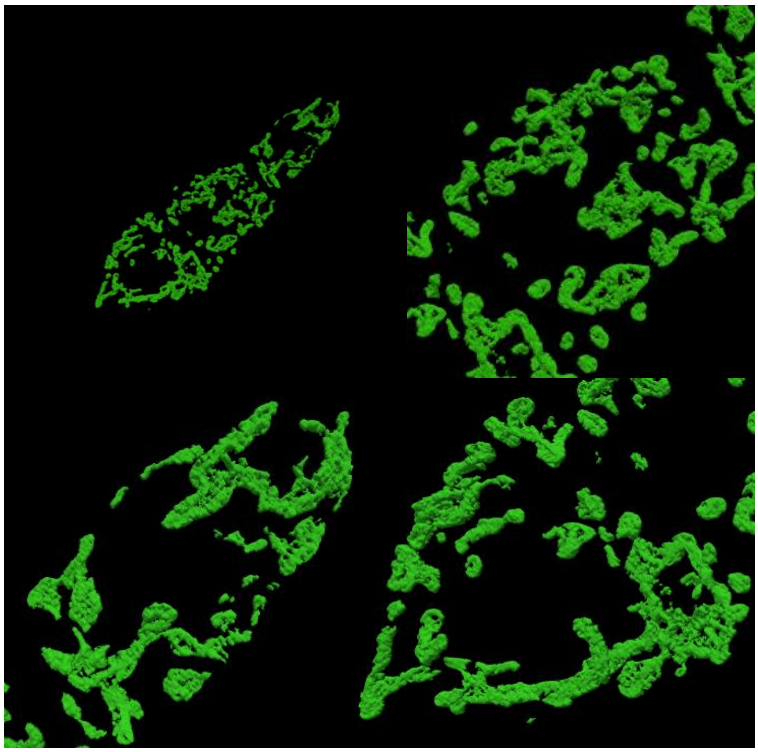
RoiSet.Zip

3. Save the ROI Drawing as RoiSet.Zip with ImageJ



MitoGraph Input

4. Run CropCell.ijm



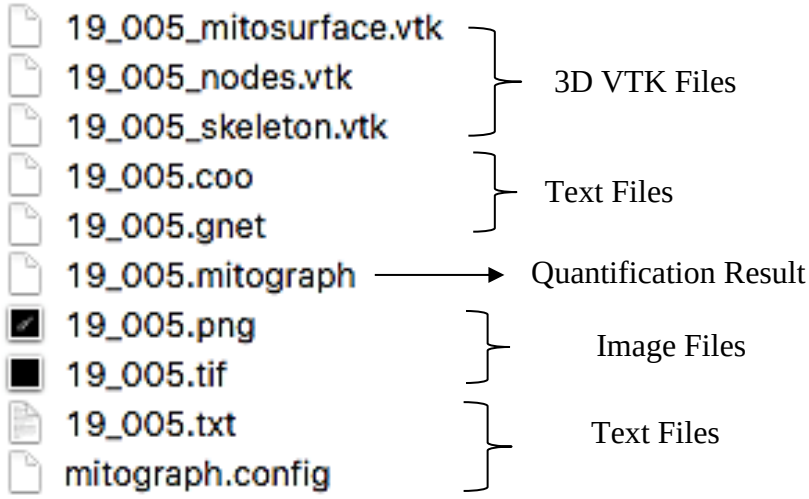
MitoGraph Output : VTK File could be opened in Paraview software (https://www.paraview.org/)

5. Run MitoGraph:

./MitoGraph -xy 0.024 -z 0.2 -rad 0.15 -scales 2.7 4.8.

45 -adaptive 2 -path ~/Desktop/Data3/cells19

Figure 3.4 The workflow of MitoGraph Software



***19_005 represent the original file name**
***All files could be opened by ImageJ, but VTK Files**

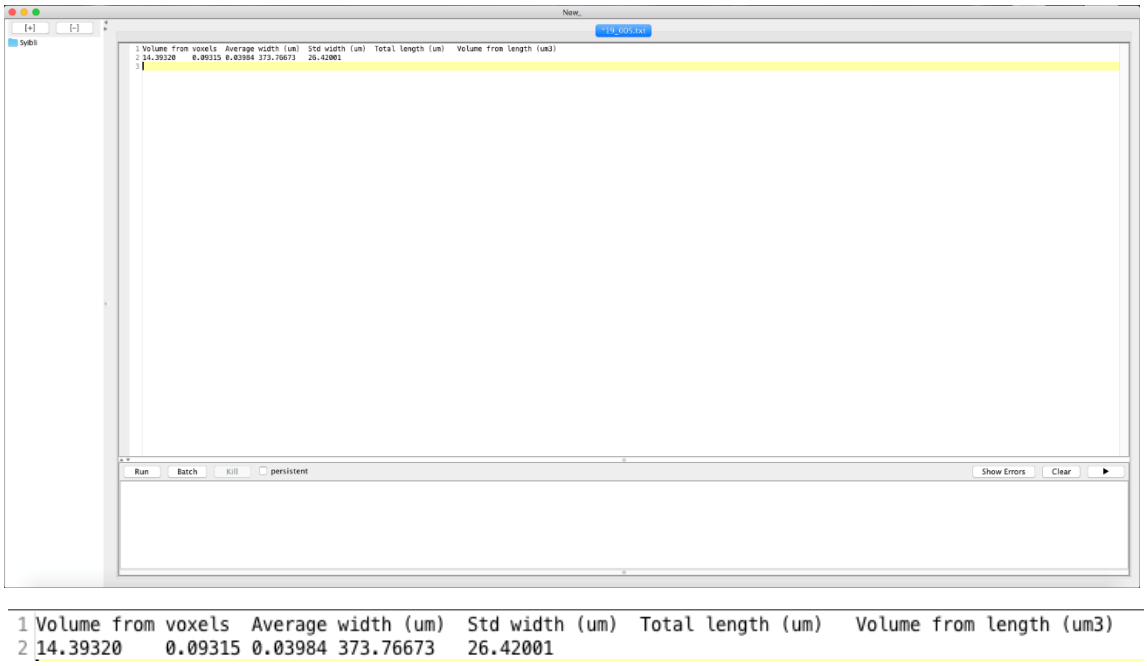


Figure 3.5 The display of MitoGraph Output and Short Explanation

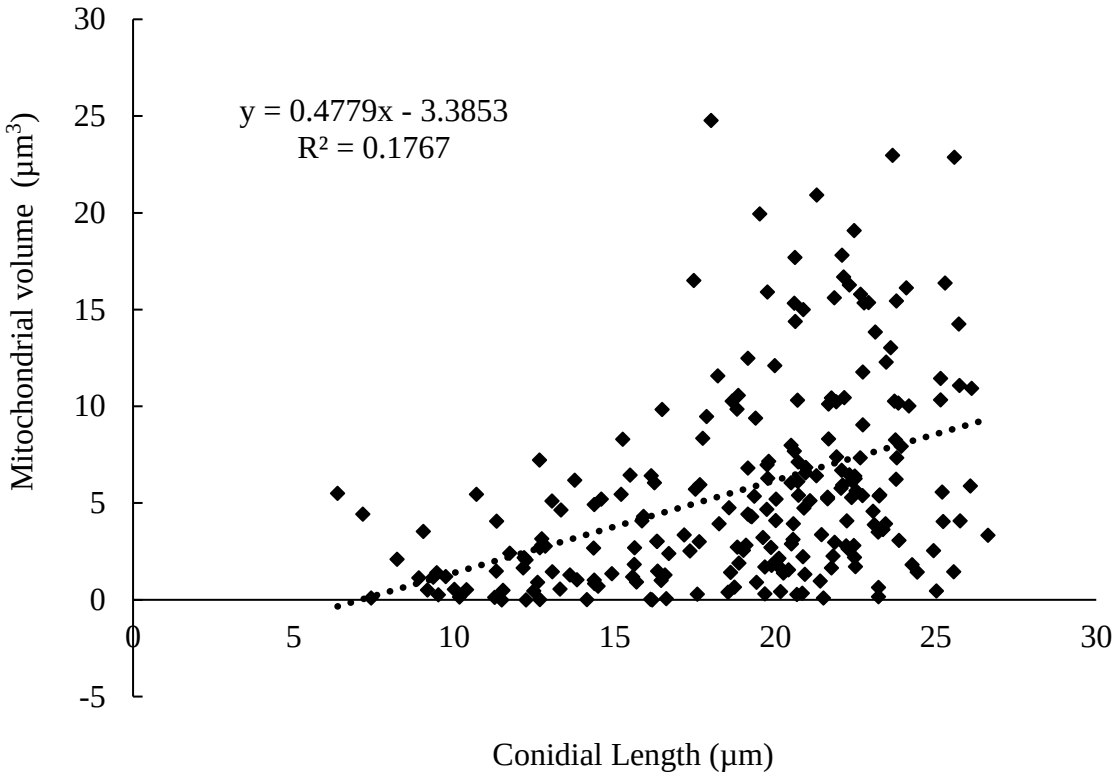


Figure 3.6 Relationship between mitochondrial volume (μm^3) (Based on voxel) and conidial length (µm)

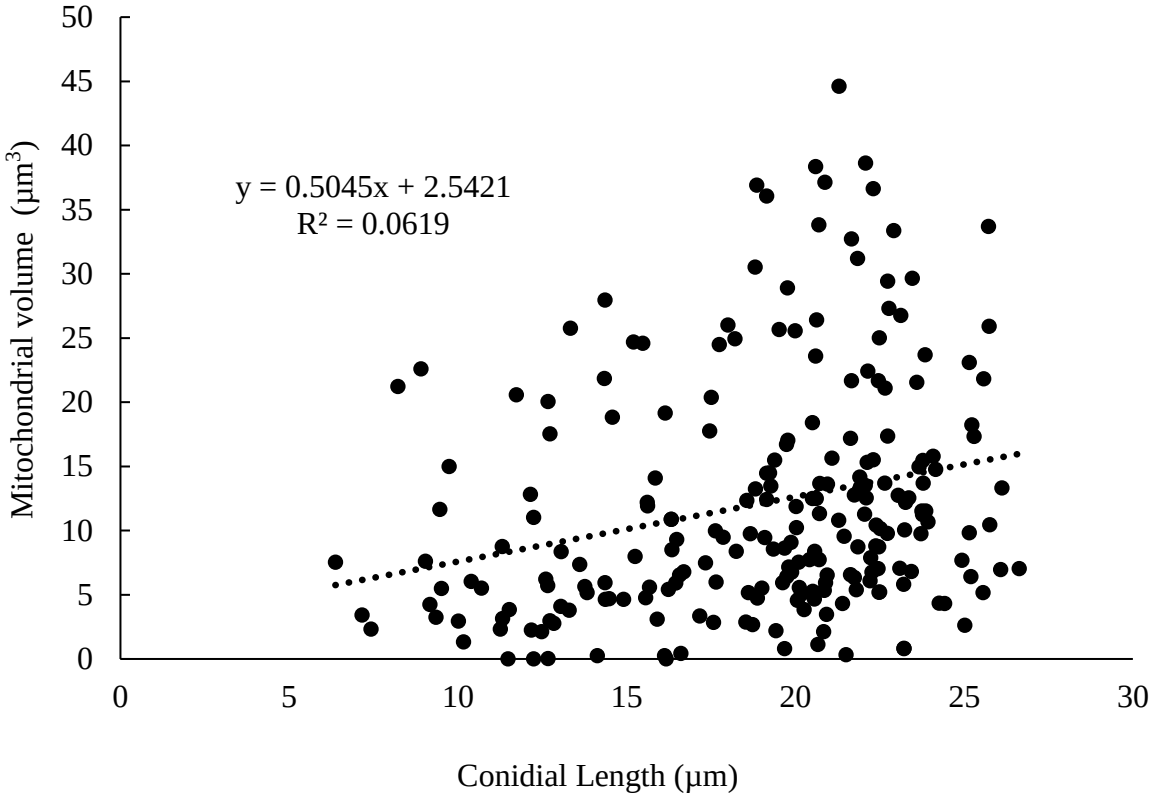


Figure 3.7 Relationship between mitochondrial volume (μm^3) (Based on length) and conidial length (µm)

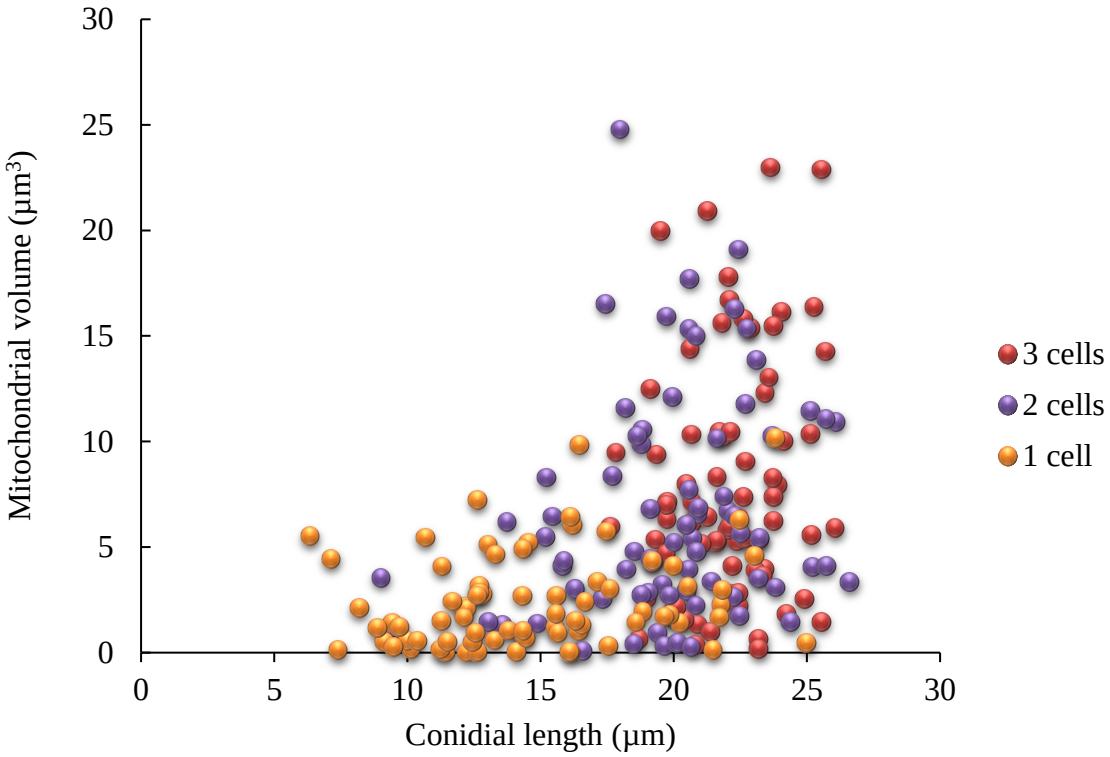


Figure 3.8 Distribution of mitochondrial volume (μm^3) (Based on voxel) in the conidia with 1 cell, 2 cells and 3 cells against conidial length (µm)

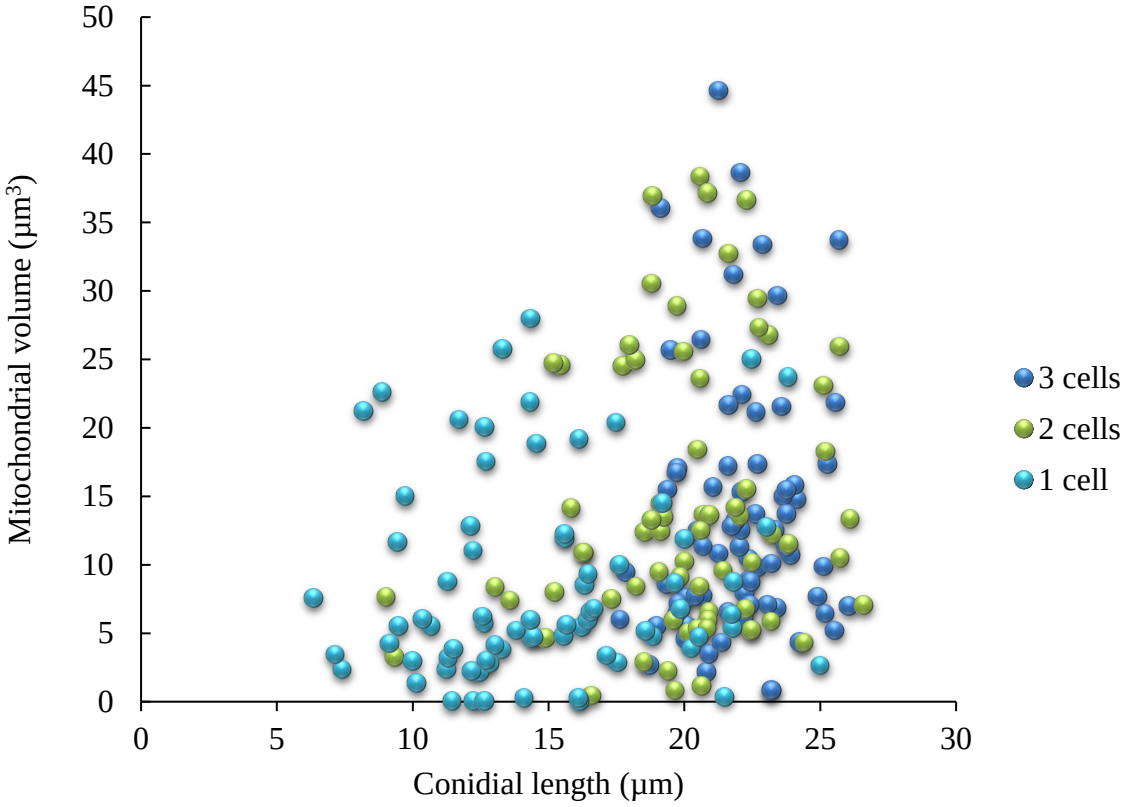


Figure 3.9 Distribution of mitochondrial volume (μm^3) (Based on length) in the conidia with 1 cell, 2 cells and 3 cells against conidial length (µm)

Chapter 4

Visualization of mitochondrial dynamics during conidia formation using slide culture-confocal microscopy

4.1 Introduction

Until now, some fungal studies including *Pyricularia oryzae*, about mitochondrial dynamics are still limited in the hyphae, because in order to observe conidia, the fungus should be incubated with a particular temperature under fluorescence light treatment, and it is a difficult effort to achieve. One of the attempts to understands the mitochondrial structure is through collecting many conidia and describe their structure as in the previous chapter. However, of course, some information is still missing.

The development of appropriate methods must be carried out to obtain images of conidia growth from one cell to three cells continuously. One of possible way to do this is to use the slide culture technique. Each researcher has the characteristics of different methods, depending on the microbes used. So many trials and error are required to get the most optimal approach. In this study, in situ observation of conidia development, together with its mitochondria, was carried out using a modified slide culture technique.

4.2 Materials and Methods

4.2.1 Slide culture technique modified with filter paper

This slide culture technique uses filter paper that was designed to supply moisture during continuous observation under a microscope. The filter paper was given oatmeal agar and inoculum of *Pyricularia oryzae* strain (CitA) -GFP. The cover glass was sealed by using petroleum jelly to trap moisture remains in the slide culture (Fig 4.1). Then, the glass slide was incubated for 4-6 days under fluorescence light with temperature 25 °C ,

and then the observation was performed using fluorescence microscopy and confocal laser scanning microscopy.

In the observation using confocal laser scanning microscopy, the objective lens was set with 100x magnification. Therefore, slide culture could be incubated for 7-8 days so that mycelium and some baby conidia already grow to attach with the wall of the cover glass. Before observing the conidia under confocal scanning microscopy, the slides were checked under fluorescence microscopy for the prospective baby conidia that would be observed.

4.2.2 Fluorescence microscopy set up

Observation under fluorescence microscopy has the purpose of capturing the conidiation event and how long the development of the formation of conidia happens. The microscope was set up with an objective lens of magnification of 20 times. Every image was captured when there was a change in conidia growth until it became mature.

4.2.3 3D image, Z stack images acquisition and confocal microscopy set up

3D and Z stack images of mitochondria were acquired by confocal microscopy Leica TCS SP8 STED 3X and Las X software using HC PL APO CS2 100x/1.40 (Oil), equipped with laser WLL (70%). Conidia were exposed by laser with excitation/emission wavelengths were 488 nm/498– 600 nm (CitA-GFP). Z stack images were set up with 256 x 256 resolution, with z step size 0.2 µm.

4.2.4 Mitochondrial distribution analysis

Mitochondrial distribution analysis was made with the observation on time-lapse of mitochondria behavior in the hyphae, the 3D image of mitochondria during conidia formation, the changes of mitochondrial volume during conidia development. Through this observation, mitochondrial behavior could be explored more deeply. Mitochondrial

volume was measured by MitoGraph software (Viana et al. 2015) and Microsoft Excel analyzed the volume result.

4.3 Result and Discussion

4.3.1 Conidia formation and time-lapse observation

Slide culture technique with modified filter paper was an established method to observe conidia formation under fluorescence microscopy. Observations on the slide culture technique showed that after conidiophores are formed, conidia took about 2.5 hours to grow from a baby until becoming matured conidia (Fig 4.2). Room temperature and moisture entrapment by closing the glass cover seem to be an essential factor for conidia development. Besides, during the observation, the room lights were also not turned off, so it was possible that the room light also supports conidia development.

Observation on hyphae shows that the mitochondria continue to move, fuse, and divided. The younger generation of hyphae, inherit mitochondria, after mitochondrial fission activity. Based on time-lapse observation, the first mitochondria in the new hyphae looks a dot-shaped. It will become more attractive, to observe mitochondria during conidia development. However, to stabilize the focus of the microscope lens on mitochondria is very difficult during conidia development. Therefore, probably it is better to make analysis on mitochondrial dynamic with 3D image of mitochondria.

4.3.2 Mitochondrial dynamic during conidia development

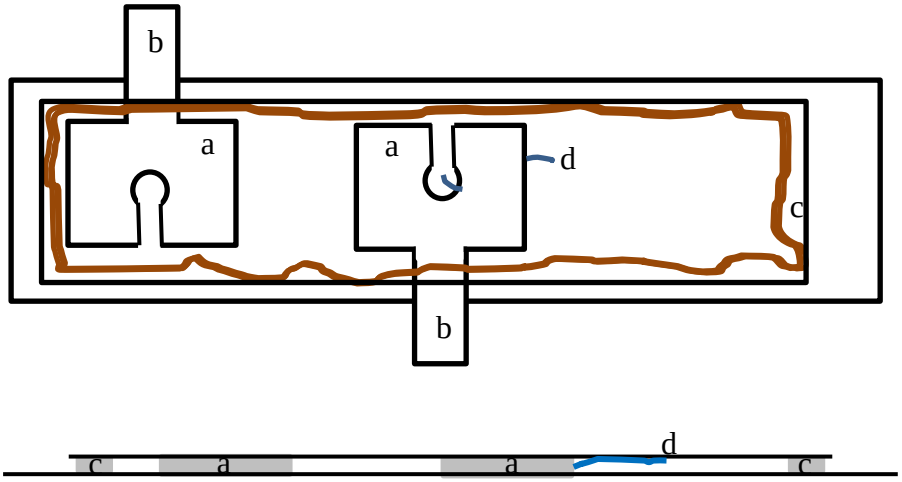
The slide culture technique with modified filter paper also allows mitochondrial behavior with a 3D image structure could be captured during conidia development under the confocal laser scanning microscopy. Z stack images also could be analyzed by MitoGraph to measure the mitochondrial volume. This experiment captures the

mitochondrial dynamic on complete and incomplete conidia. the conidium was called incomplete because it only develops until 2 cells (Fig 4.6).

Based on the 3D image result, both in the complete and incomplete conidia, mitochondria develop to become a network-shaped. From single-cell conidia, mitochondria have become a network-shaped, but look denser, then fragmented and become a wider network, with the increase of conidia age (Fig 4.4). In this observation, still, there is missing information, that is mitochondrial dynamic from conidiophore to baby conidia. Observation of mitochondrial dynamics, when in a conidiophore until becoming a single cell conidium, is also critical to note. So that it can be concluded more clearly how mitochondria distribute theirself in the initial conidia. The obstacle in this observation is the opportunity to observe a conidiophore that will turn into conidia at a magnification of 100 times requires several trials and error again.

During the conidia development, some mitochondria disappear (Fig 4.4 No 7 and 8). This result is in accordance with mitochondrial volume analysis since single cell-conidia until matured conidia, both conidia has mitochondrial volume changes. The value decreased with the increase of conidia growth (Fig 4.5; Fig 4.7). This possibility is a mitophagy event, according to Zhong (2016) mitochondrial fission influences the conidiation of *P. oryzae*.

Interestingly, after several times of decreasing mitochondrial volume, there is a moment when mitochondrial volume increases again. This phenomenon happens in the incomplete conidia. From the 3D image, it shows that mitochondria grow back (Fig 4.7; Fig 4.6 No 24-33). Therefore, it would probably also happen in complete conidia if the observation was continued.



a. Filter paper + oatmeal agar + fungal inoculum
b. Area for SDW droplet
c. Petroleum Jelly
d. Fungal mycelium



Fig. 4.1 Slide Culture Technique with modified filter paper

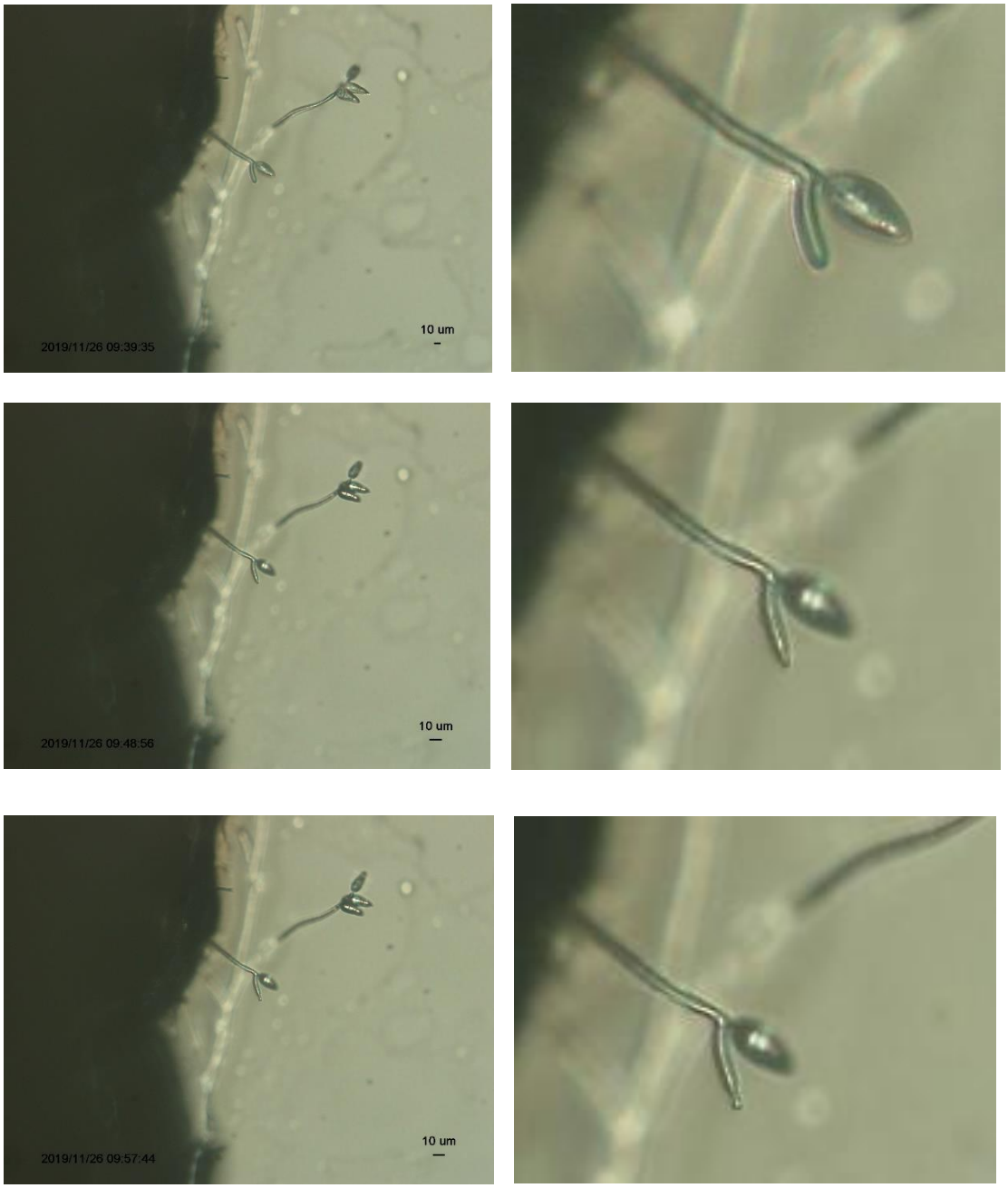


Fig. 4.2 Conidia development from conidiophore

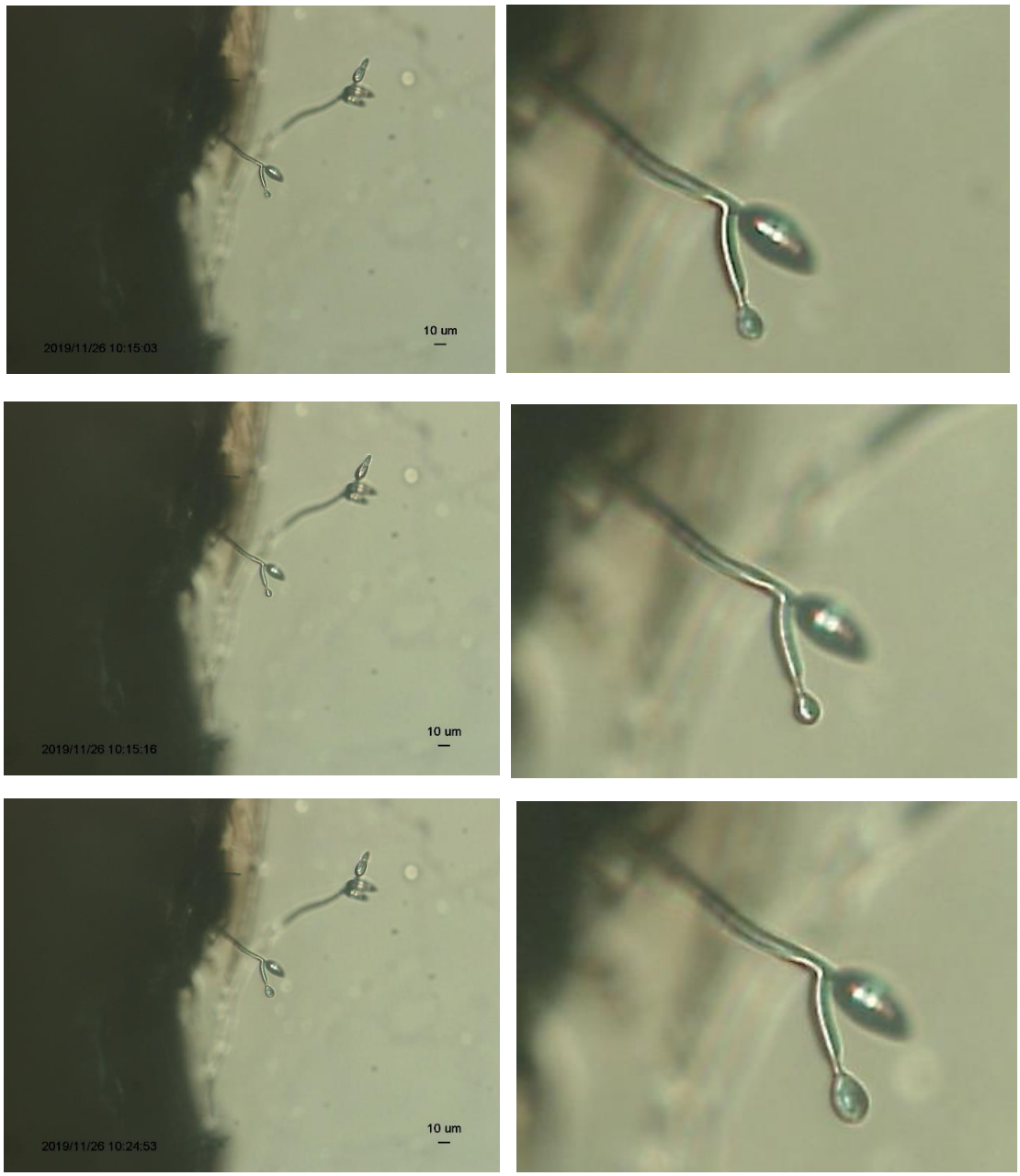


Fig. 4.2 Conidia development from conidiophore *(continued)*

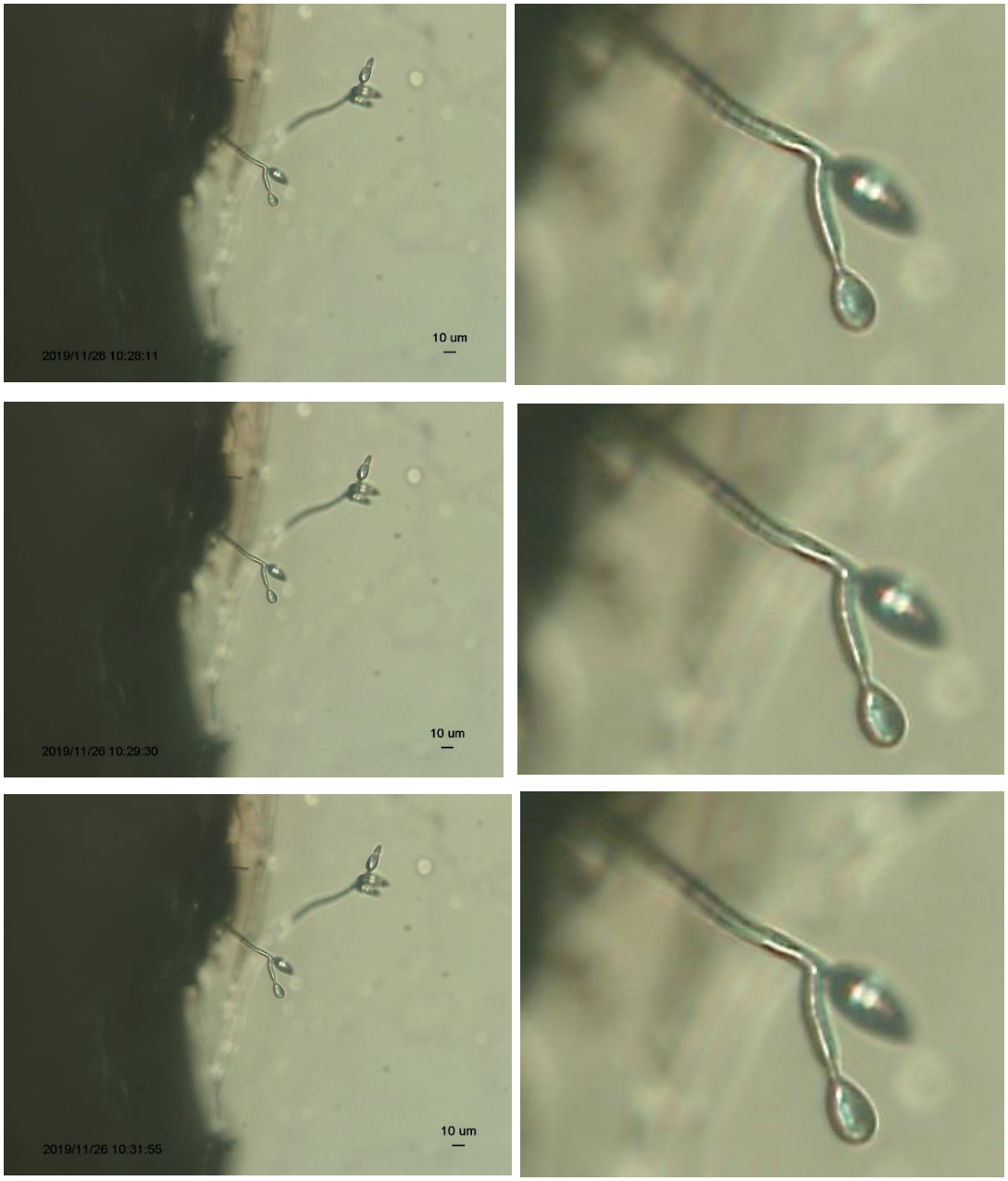


Fig. 4.2 Conidia development from conidiophore *(continued)*

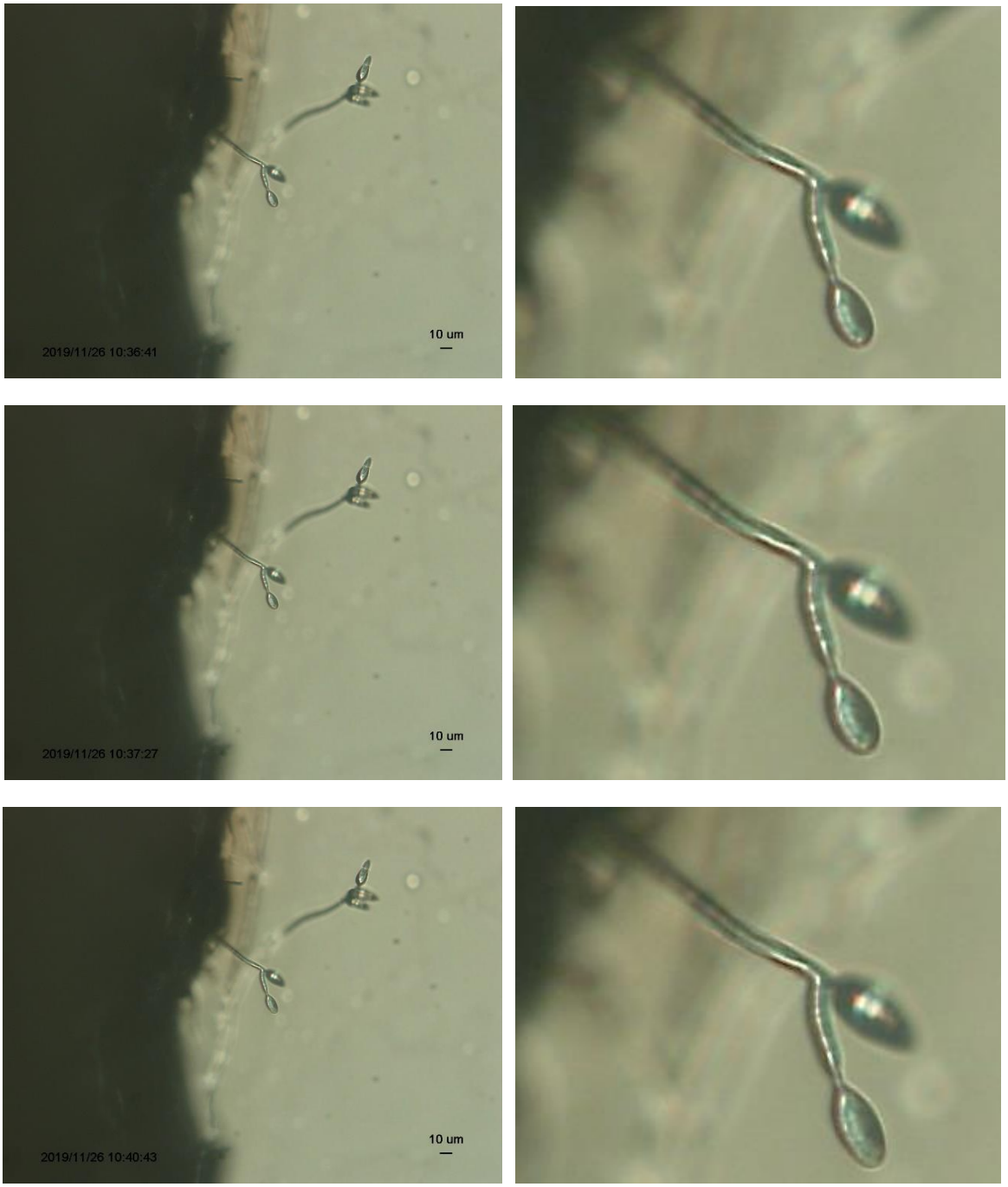


Fig. 4.2 Conidia development from conidiophore *(continued)*

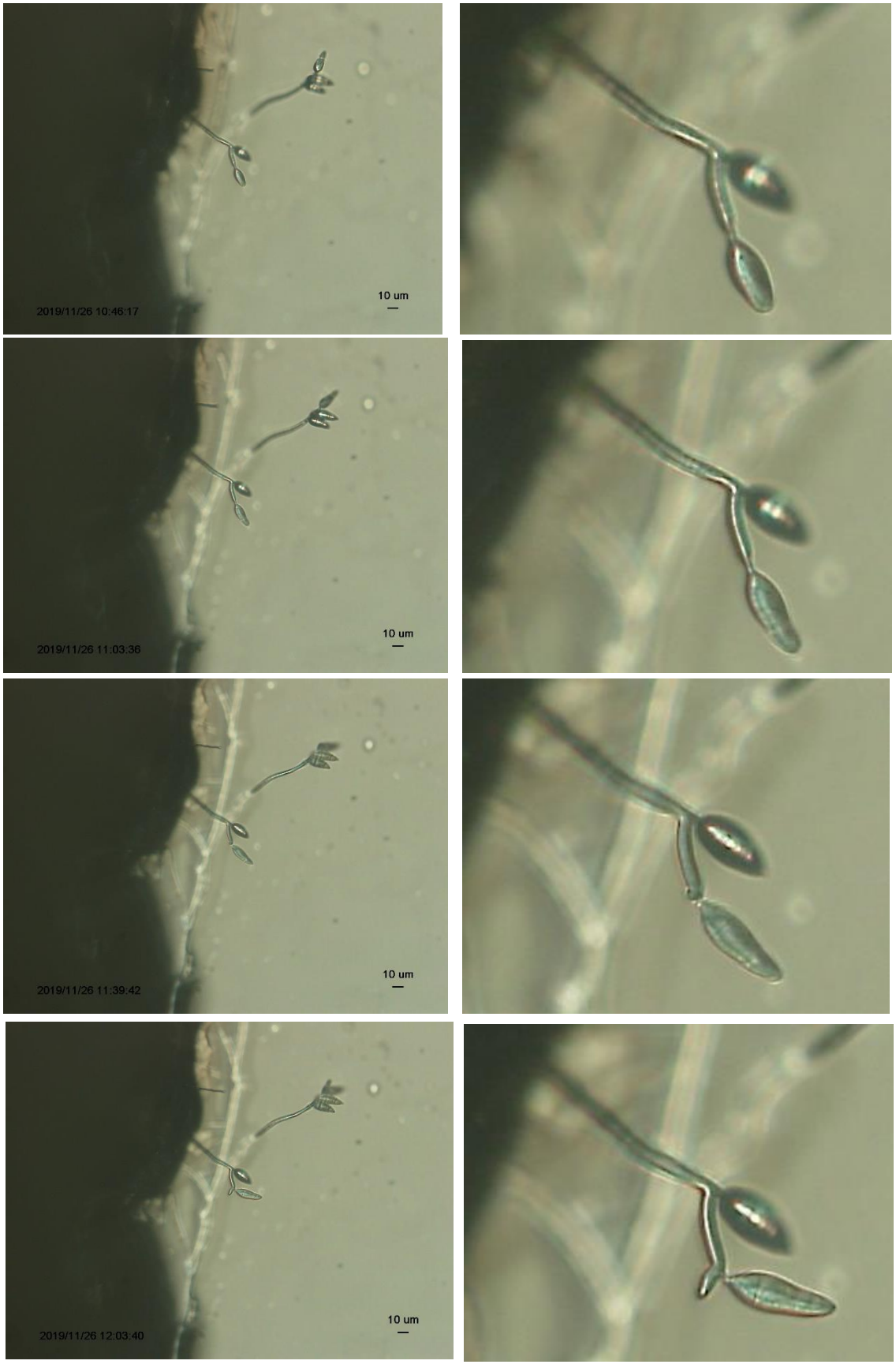


Fig. 4.2 Conidia development from conidiophore *(continued)*

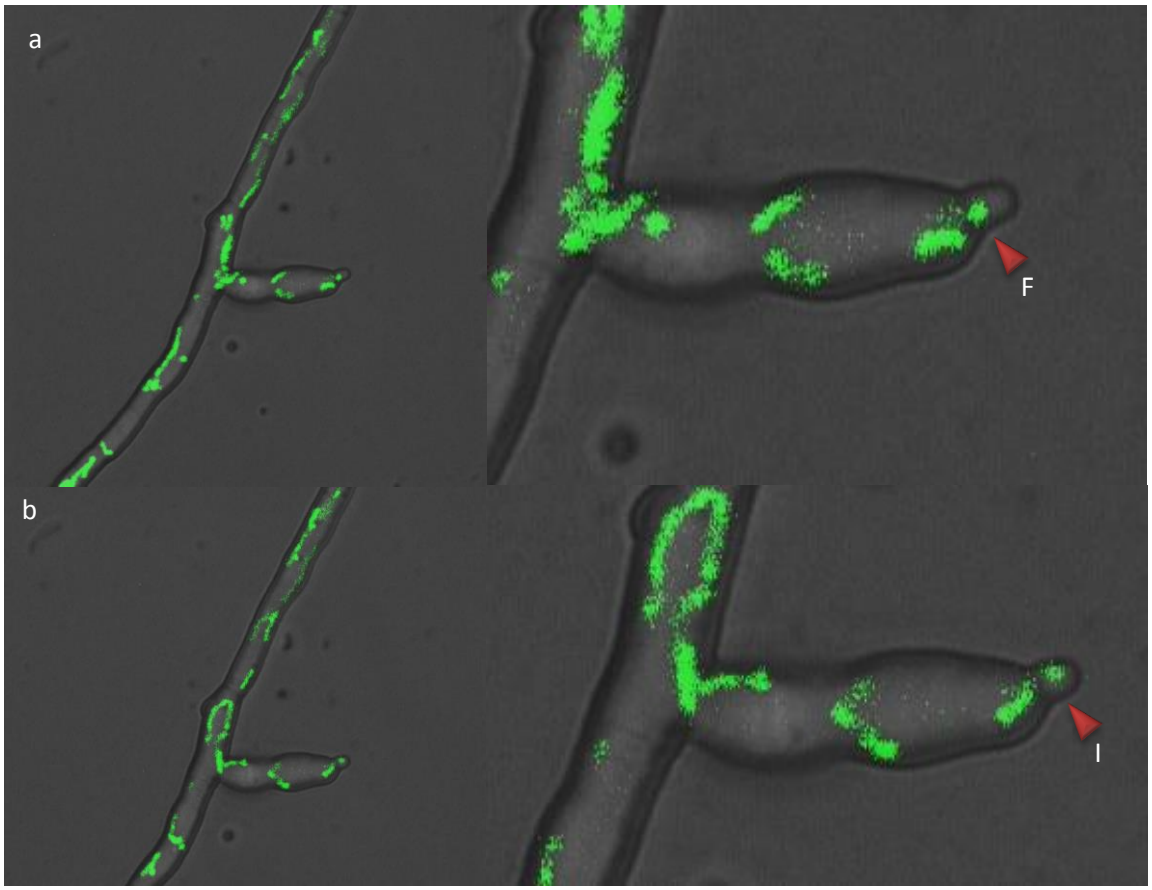


Fig. 4.3 Time lapse of mitochondrial behavior in the hyphae of *Pyricularia oryzae*. Mitochondrial activity in the hyphae (a) (b); Mitochondrial fission (Arrow F); Mitochondrial inheritance in the young hyphae

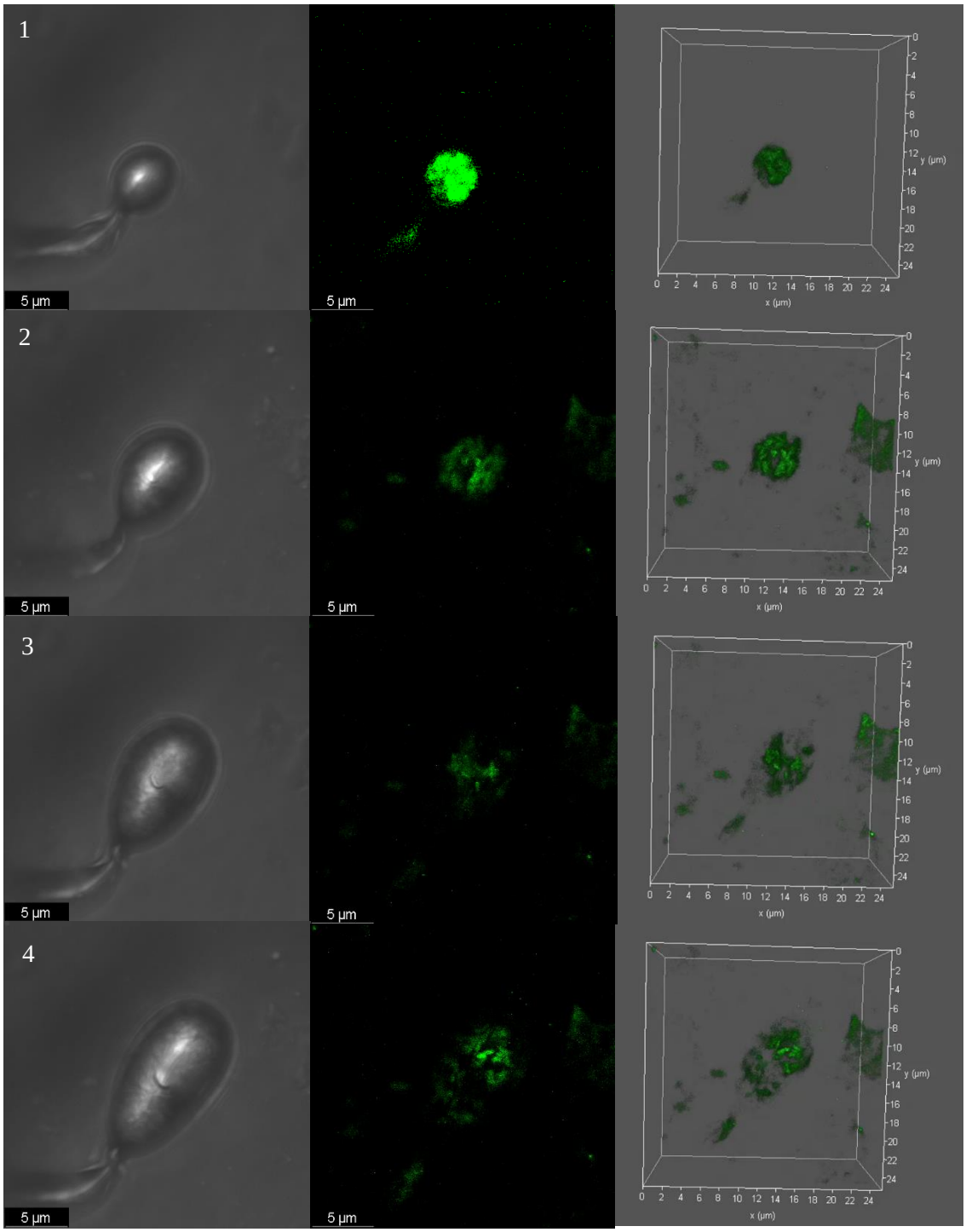


Fig. 4.4 Complete conidia and mitochondria development

(Sample1)

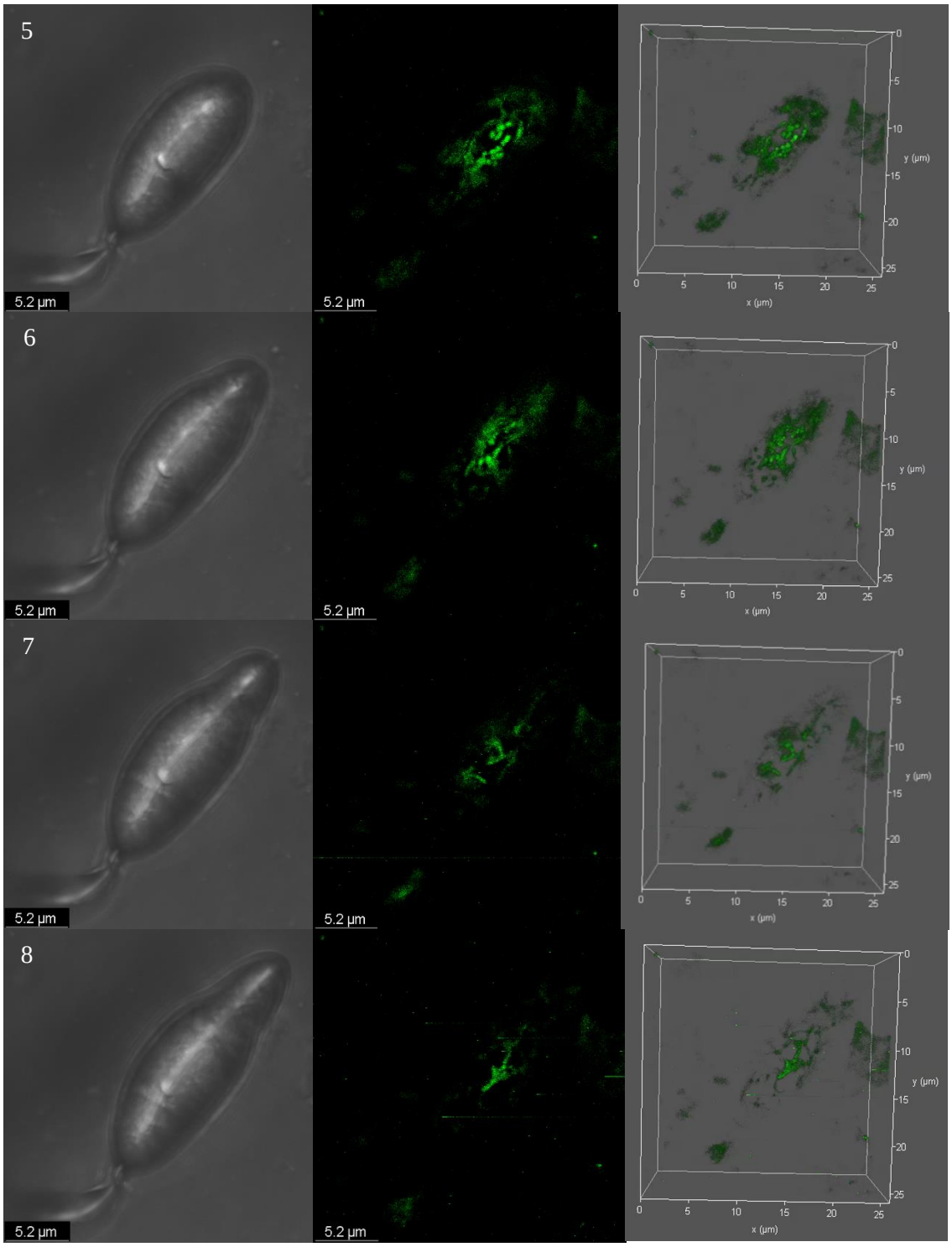


Fig. 4.4 Complete conidia and mitochondria development

(Sample1) *(continued)*

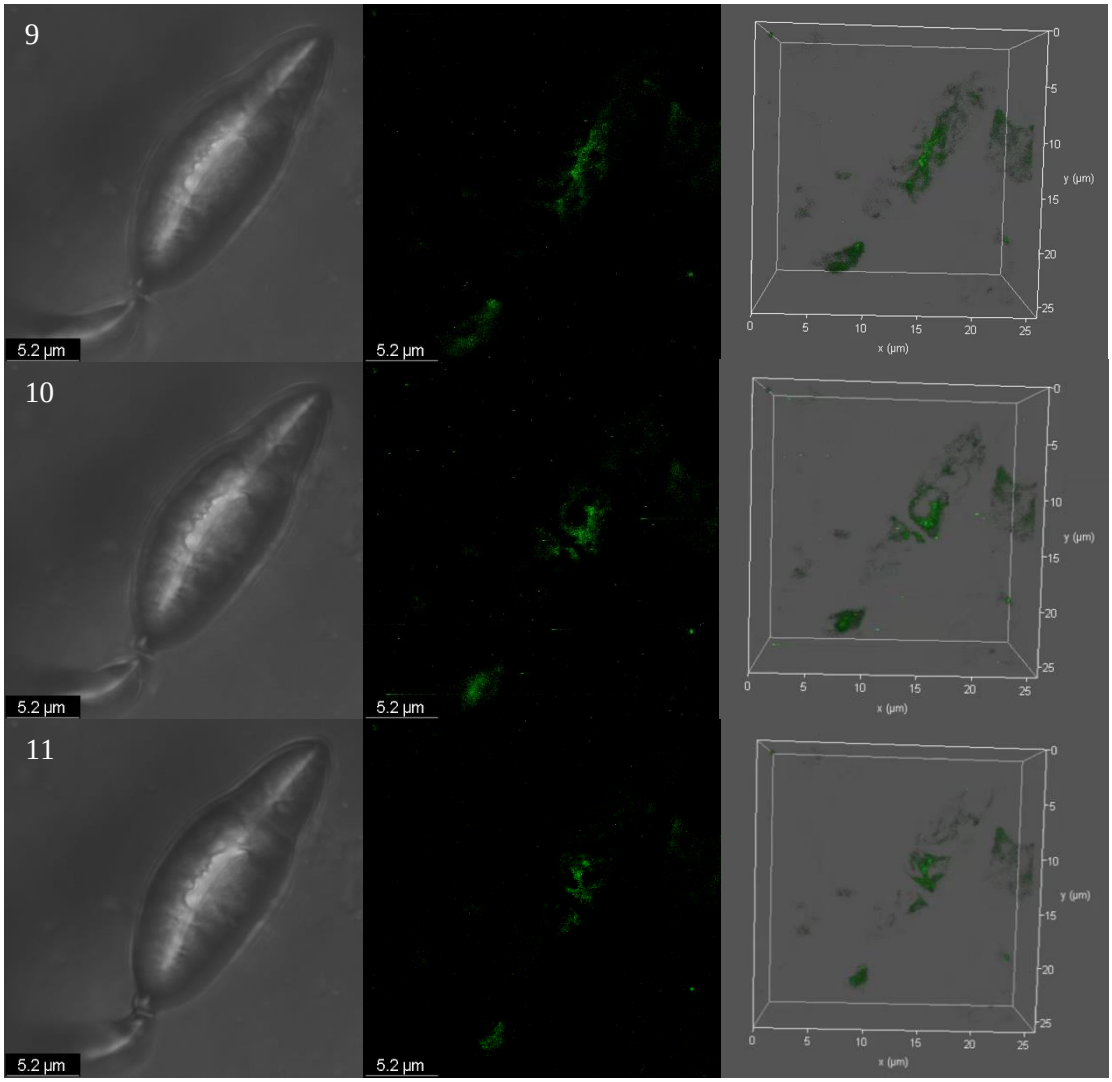


Fig. 4.4 Complete conidia and mitochondria development

(Sample1) *(continued)*

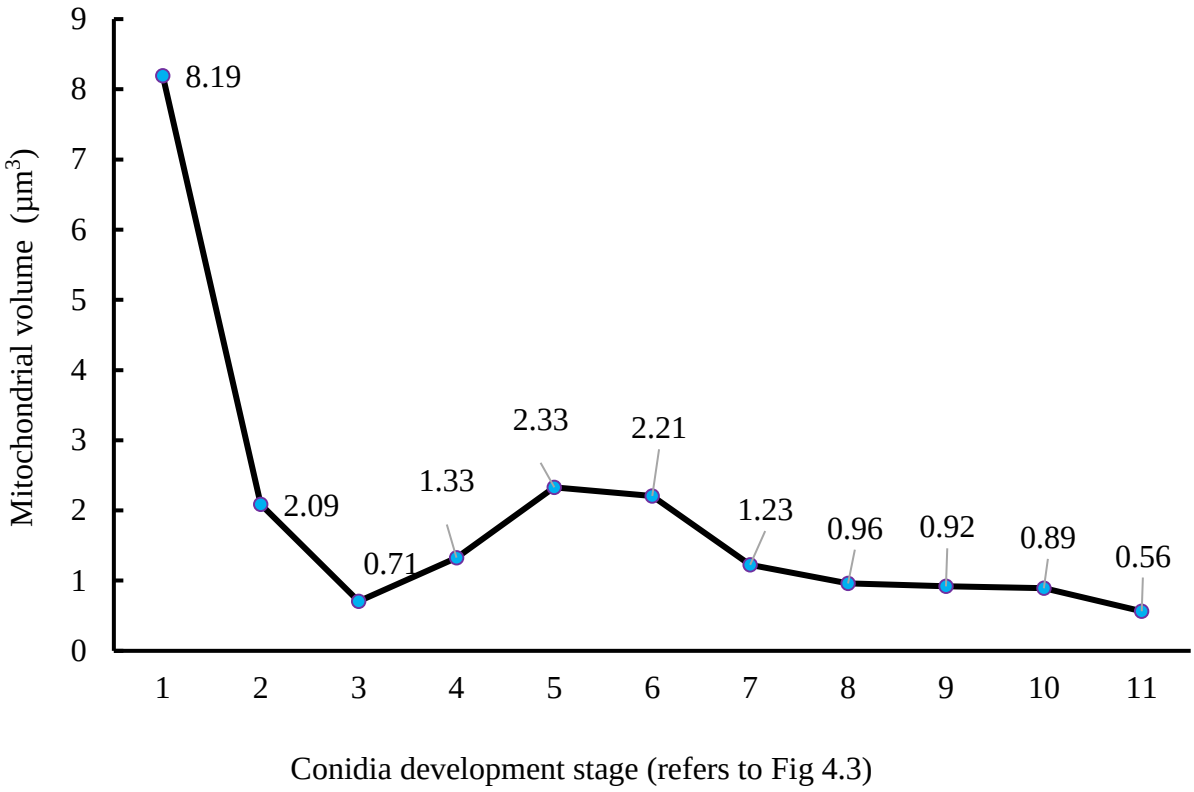


Fig 4.5 The changes in mitochondrial volume during conidia development (Sample 1)

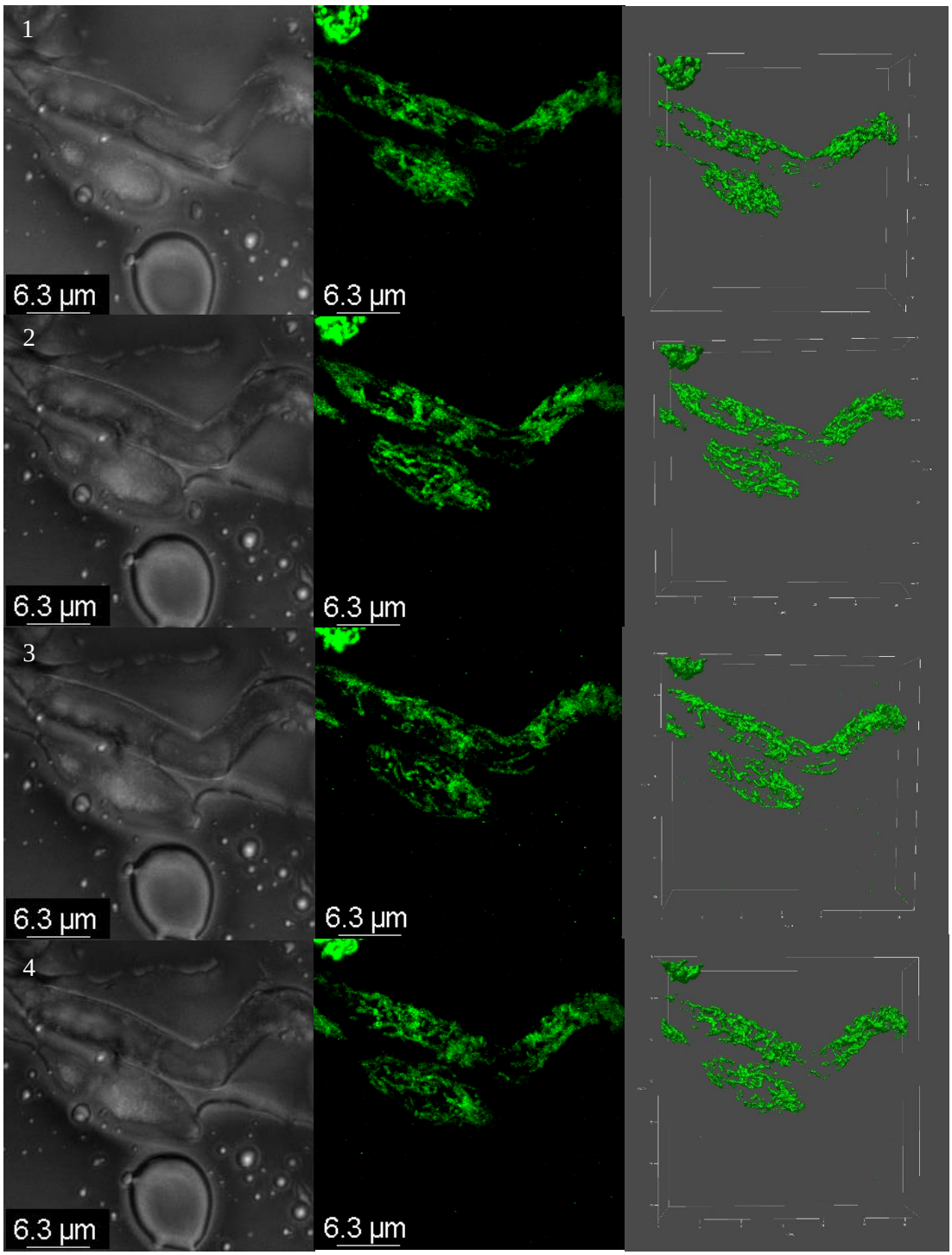


Fig. 4.6 Incomplete conidia and mitochondria development

(Sample 2)

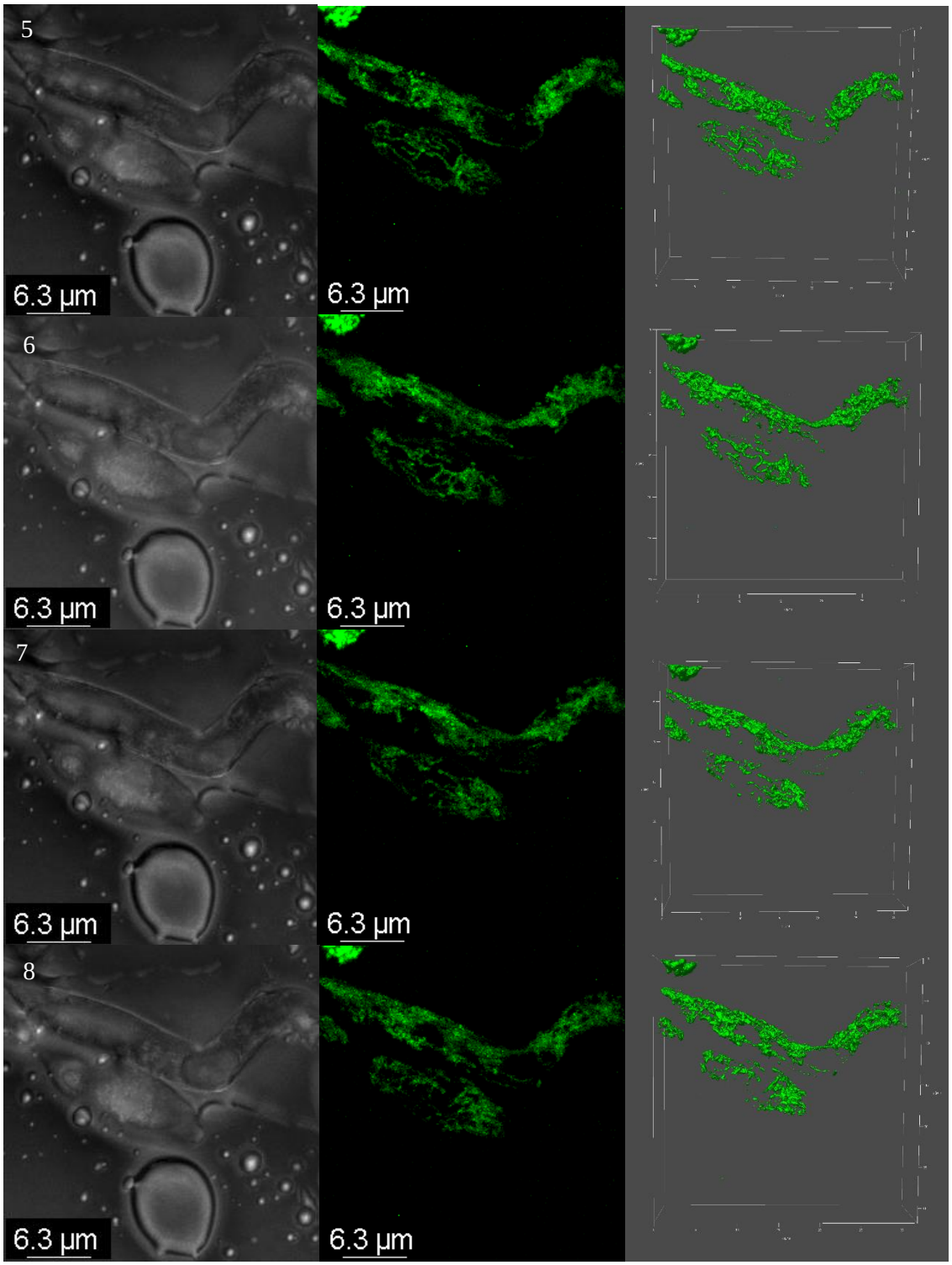


Fig. 4.6 Incomplete conidia and mitochondria development

(Sample 2) *(continued)*

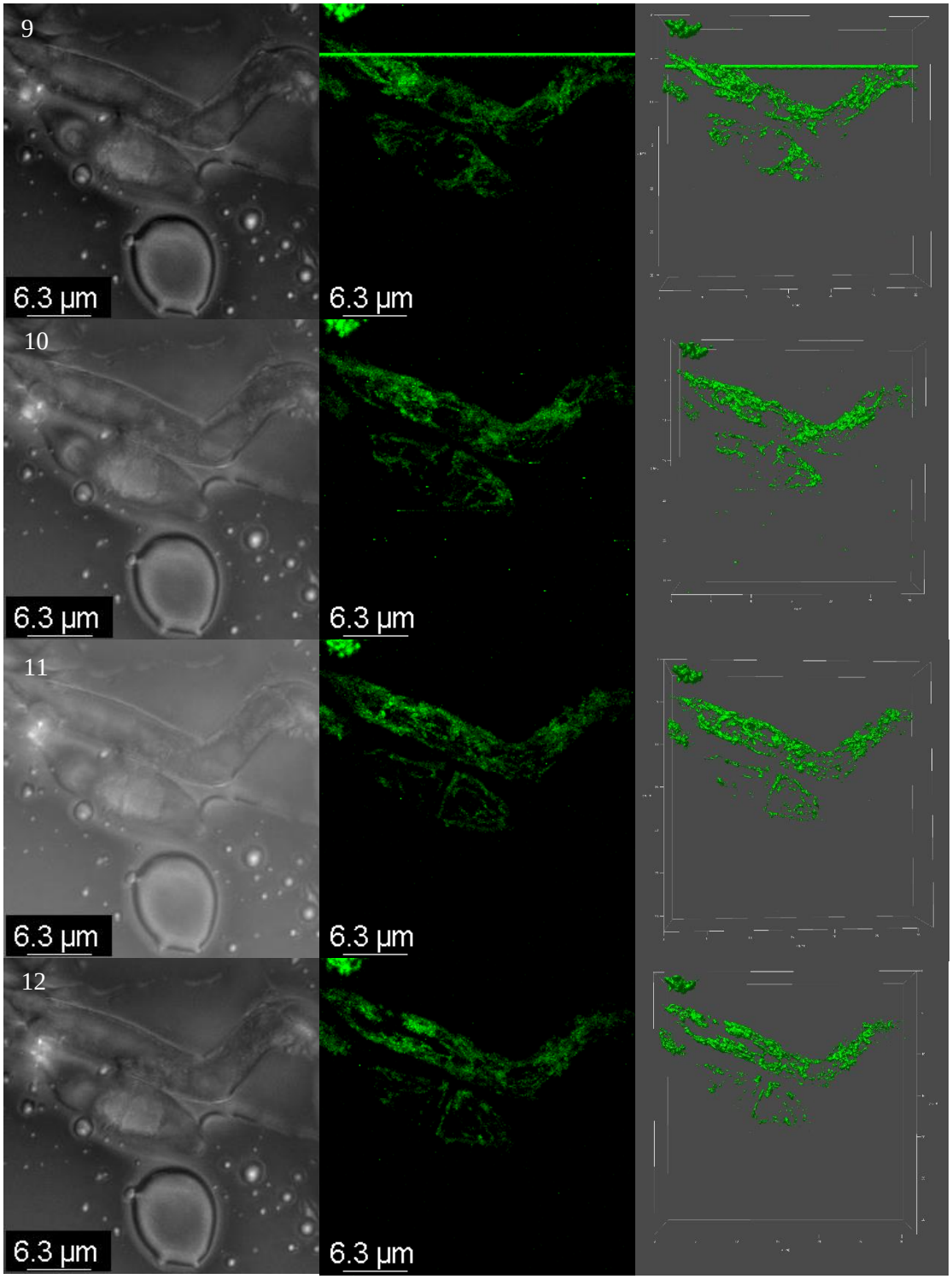


Fig. 4.6 Incomplete conidia and mitochondria development

(Sample 2) *(continued)*

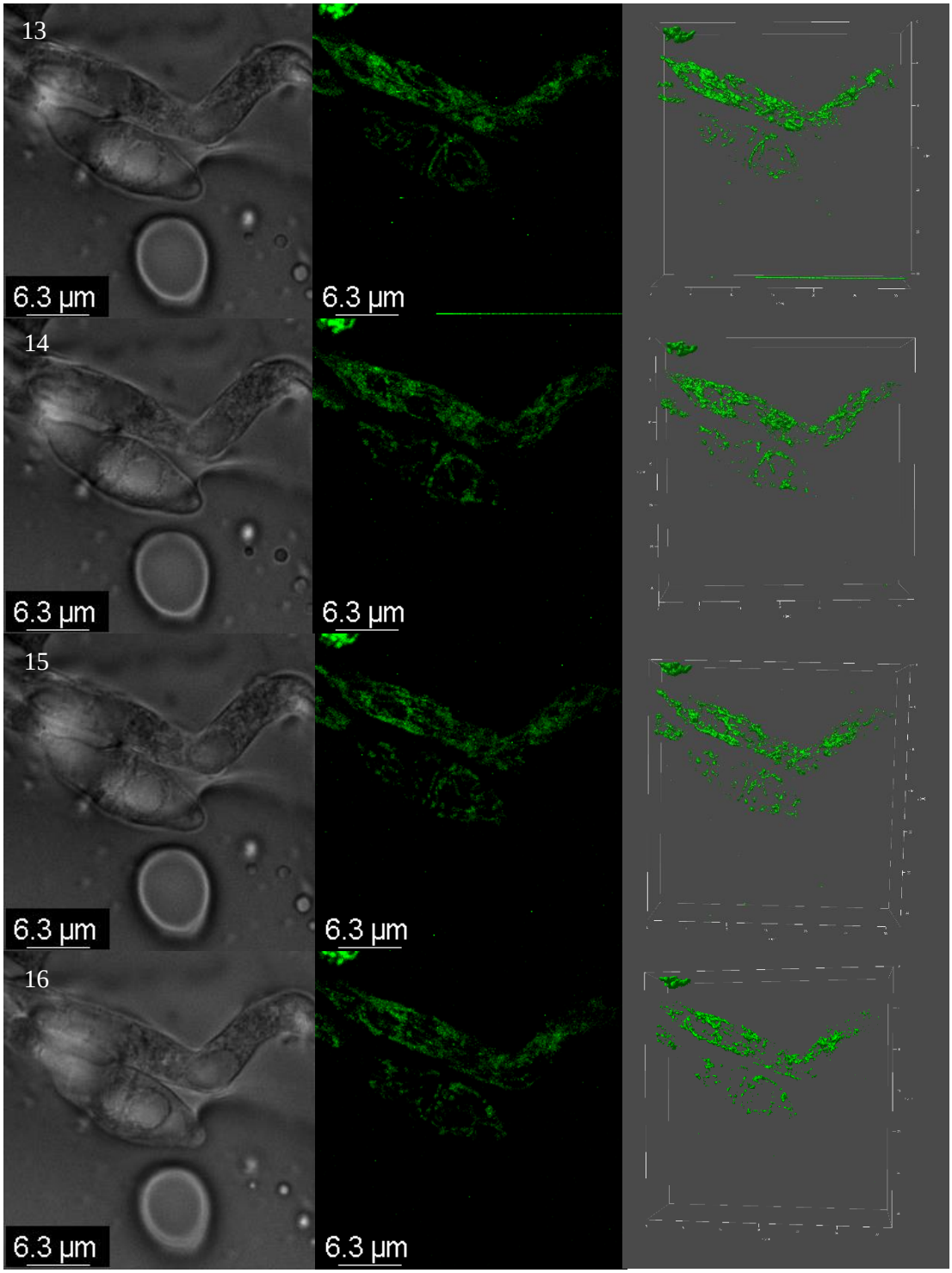


Fig. 4.6 Incomplete conidia and mitochondria development

(Sample 2) *(continued)*

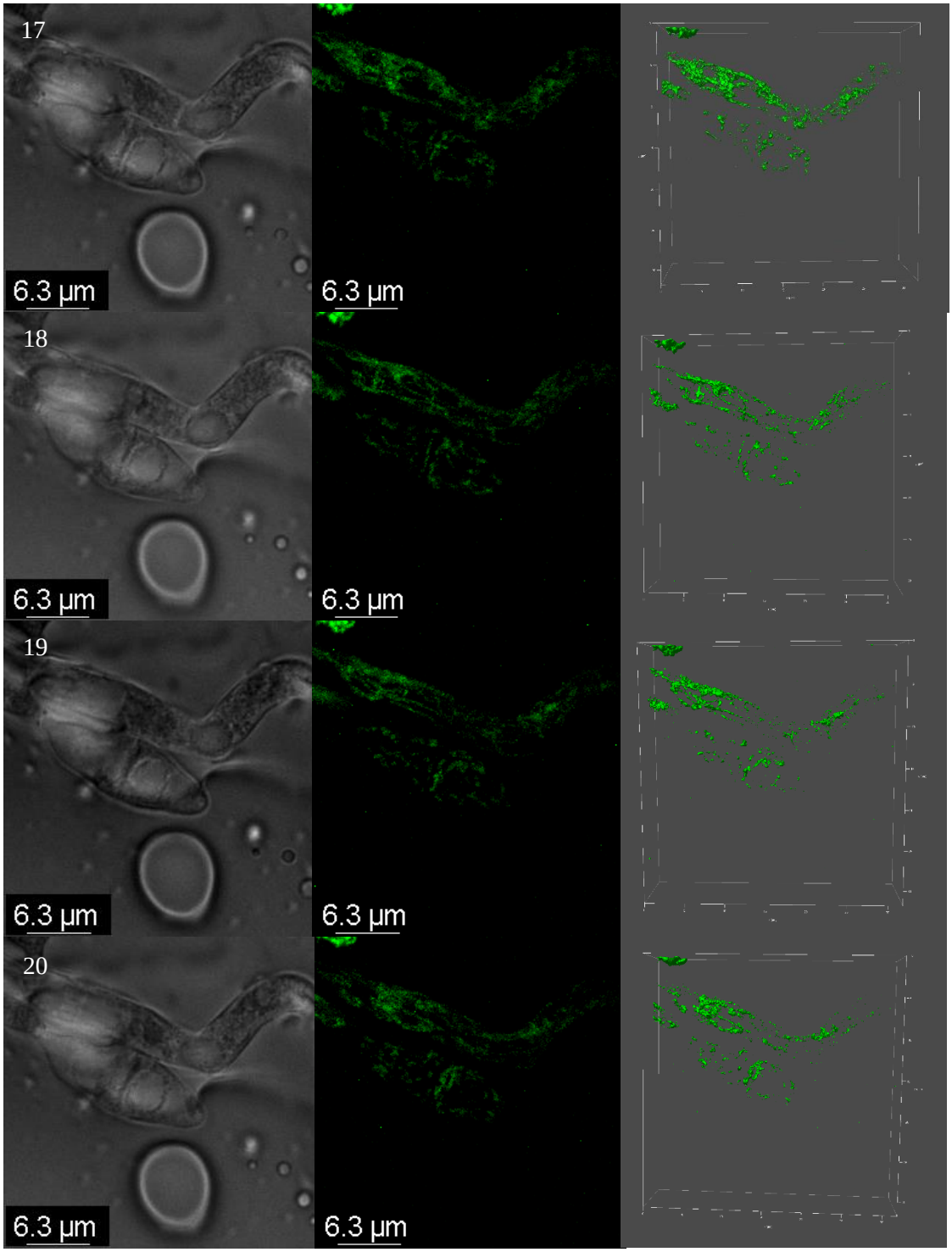


Fig. 4.6 Incomplete conidia and mitochondria development

(Sample 2) *(continued)*

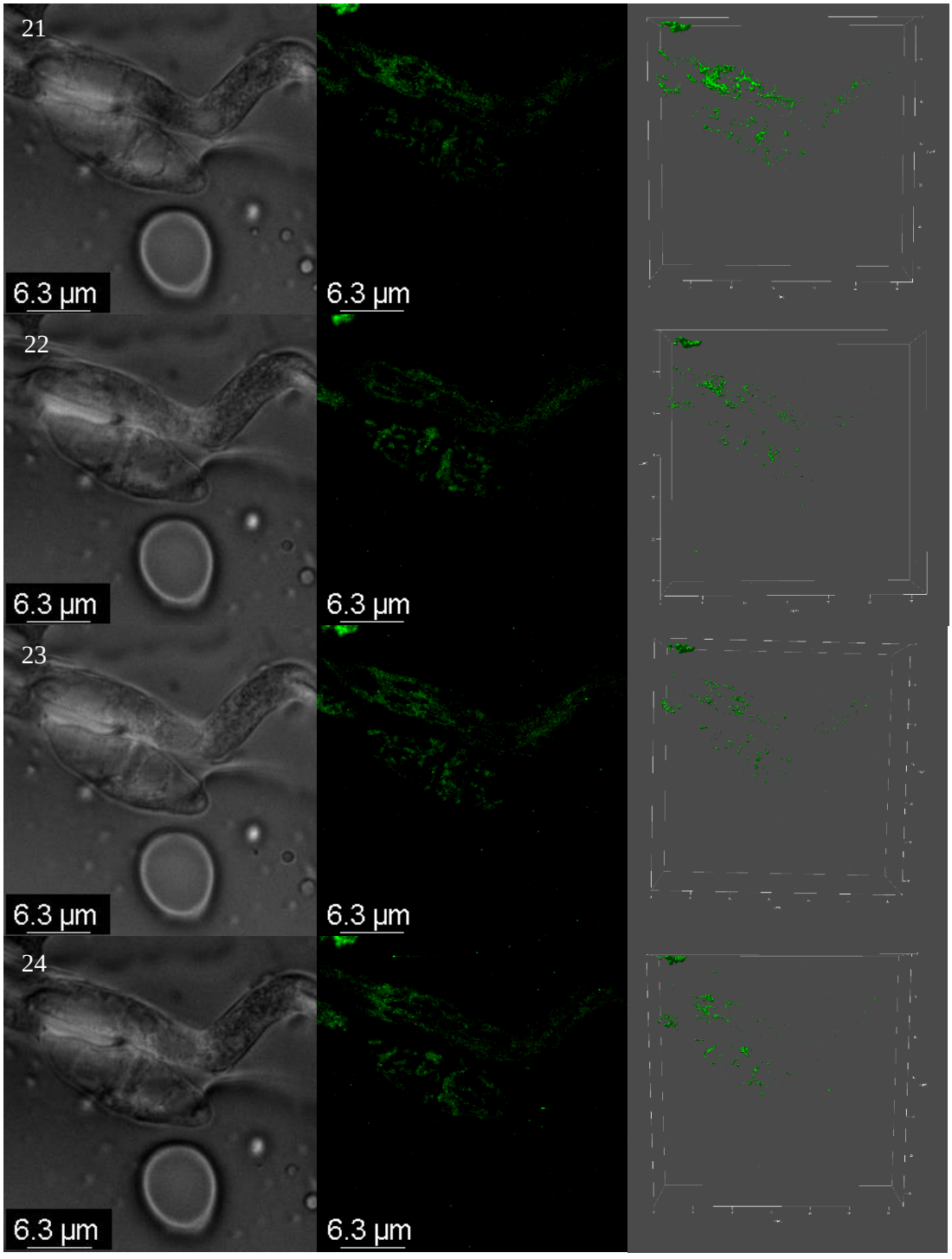


Fig. 4.6 Incomplete conidia and mitochondria development

(Sample 2) *(continued)*

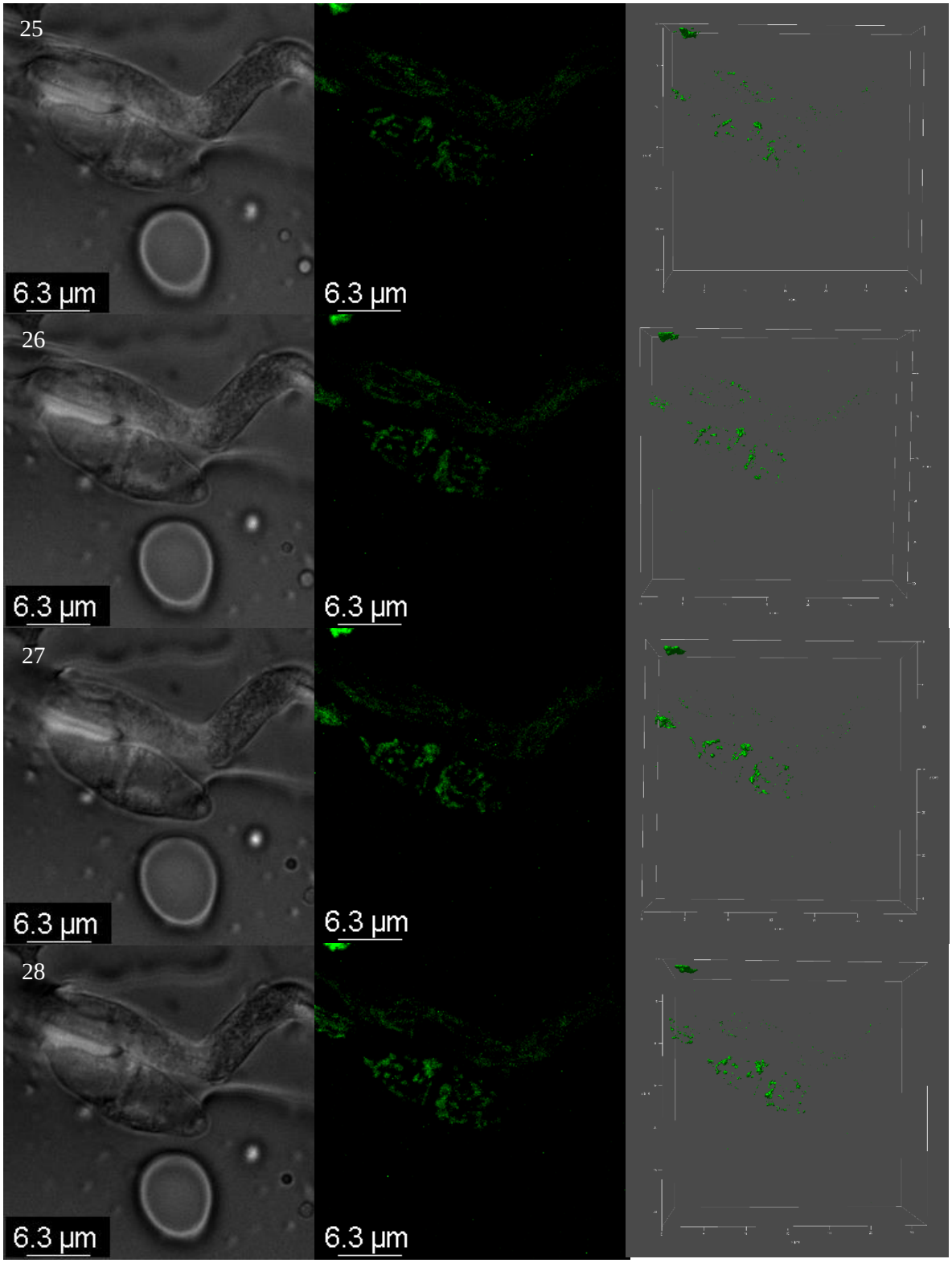


Fig. 4.6 Incomplete conidia and mitochondria development

(Sample 2) *(continued)*

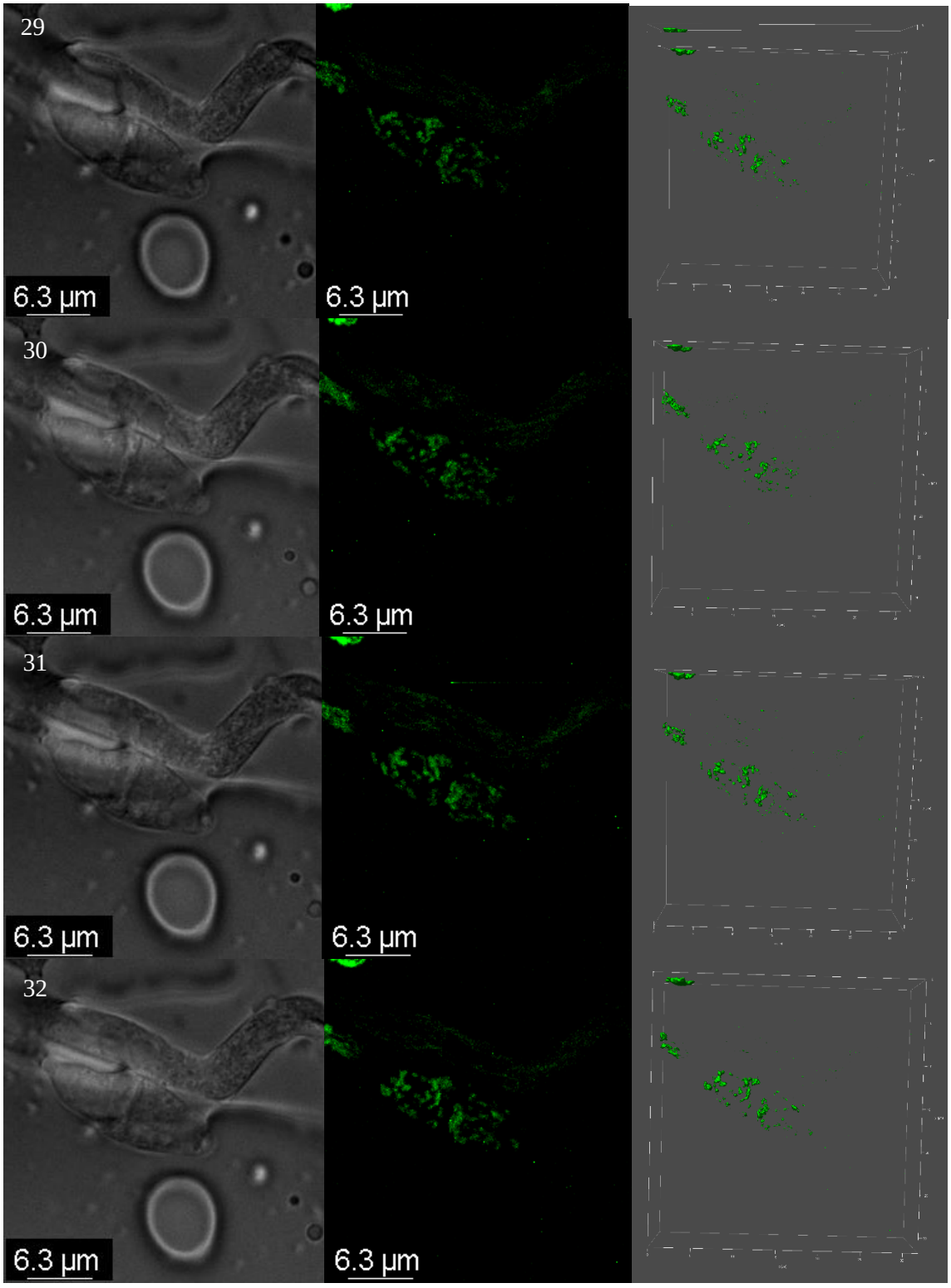


Fig. 4.6 Incomplete conidia and mitochondria development

(Sample 2) *(continued)*

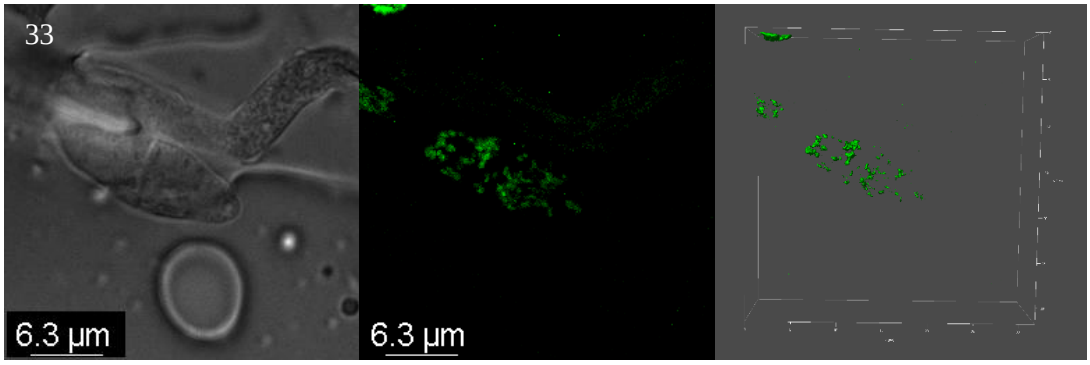


Fig. 4.6 Incomplete conidia and mitochondria development

(Sample 2) *(continued)*

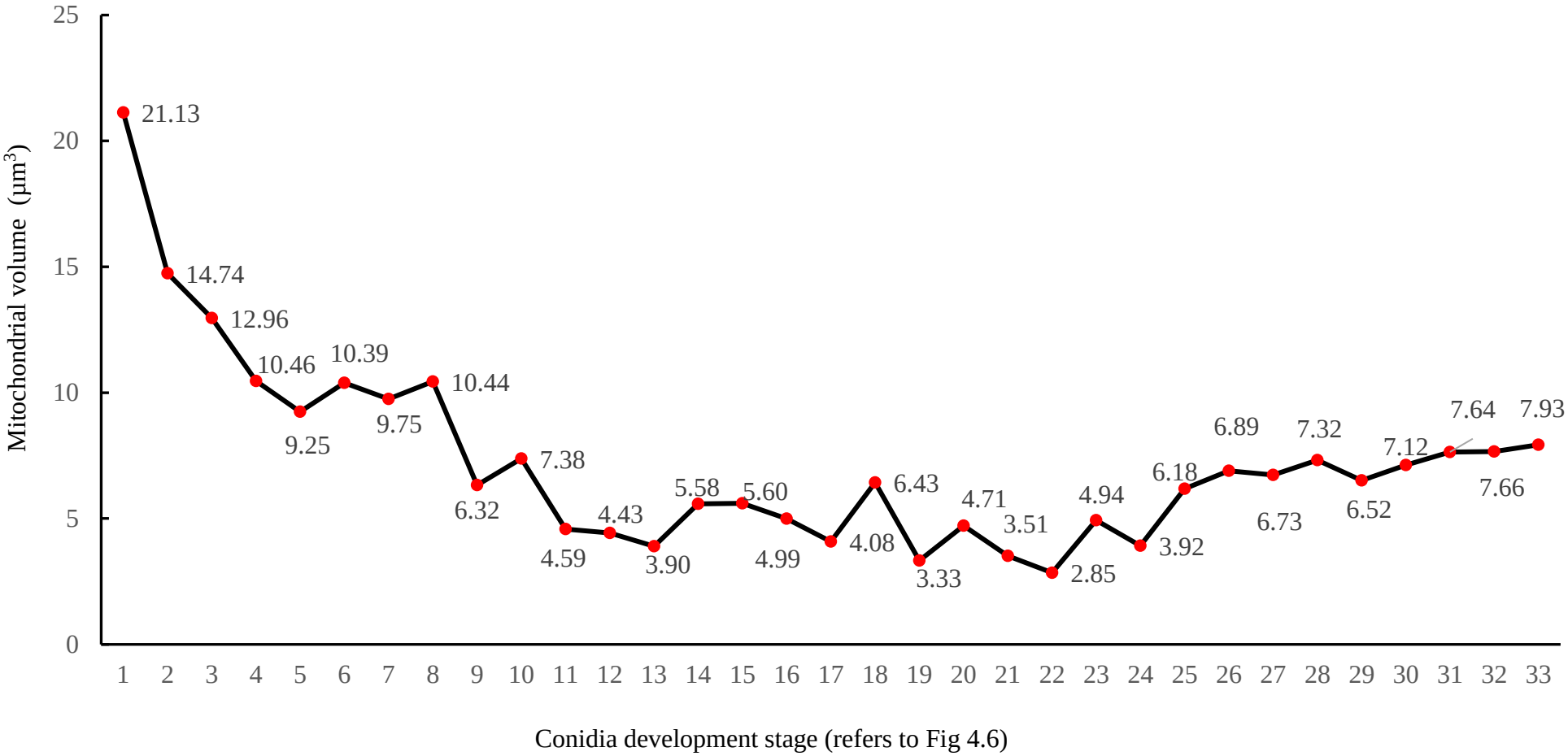


Fig 4.7 The changes in mitochondrial volume during conidia development (Sample 2)

Chapter 5

General Discussion

The problem of resistance in *Pyricularia oryzae* due to the application of QoI fungicides is a problem that should be studied carefully. Mainly, solving the question of how the mechanism of mutating mitochondria causes resistance to this fungus. The initial approach is to understand that there is a defensive structure of *P. oryzae* that can cause an explosion of rice blast disease, which is conidia. By following this fundamental information, basic knowledge about mitochondrial inheritance to conidia becomes very interesting to be explored.

Two things have to be known — first, the behavior of the conidial mitochondria and second, how to visualize mitochondria properly. So, the activities of the mitochondria can be studied. This study used *P. oryzae*, which had been transformed using (CitA)-GFP. (CitA)-GFP is a plasmid that would transform the nucleus to produce citrate synthase protein in the ribosomal cytoplasm that has been attached to Green Fluorescence Protein. This protein is needed in the process of the Kreb cycle in the mitochondria, so that the presence of the citrate synthase protein that has been attached by GFP, causes the mitochondria to express green color under fluorescence microscopy. The results of this transformation had been confirmed using MitoTracker, that the coloring by MitoTracker is at the same location as the green expression caused by (CitA)-GFP.

After that, the research is carried out by identifying the optimal time to get conidia with one cell, two cells, and three cells. In general, one cell is considered as a baby conidium, while two cells are considered as young conidia and three cells as matured conidia. But interestingly, although the optimal time was found was 36 hours after

incubation, conidia were still found with a single cell and two cells after incubation 72 hours. It seems that most of the conidia of babies turn into adults, while a small proportion of conidia remains in the condition as single cells or two cells.

In the second experiment, conidia collection after fungal culture was incubated for 36 hours. The conidia that have been collected are then observed for their mitochondrial structure. It should be noted that this culture is a fungal culture that had been aged 2 weeks and washed to clean the entire initial colony so that the conidia that were harvested after 36 hours of incubation are fresh conidia that are just grown by conidiophores. The observation result of the mitochondrial structure is quite surprising because 76% of the single-cell conidia have network-shaped mitochondria and only 14.67% are dot-shaped. This result needs to be reconfirmed by looking at the development of mitochondria from baby until matured conidia, continuously. Based on this result, it might be possible that conidia with a single cell which was originally thought to be young conidia, actually were matured conidia without septa formation.

Seeing how the development of the first and second research results. The next research was trying to quantify mitochondria based on their volume and analyze the results. From all of the z stack images that have been collected from conidia with one cell, two cells, and three cells, they were then processed by using MitoGraph software to see their mitochondrial volume. Then, the analysis was done to examine the relationship between conidial growth and mitochondrial development. The results of the regression analysis only produced a relationship value of 17% and 6%. Therefore, it was concluded that the development of mitochondria was out of sync with the growth of conidia.

To explore more information about this phenomenon, observations were made continuously during the development of conidia from one cell to three cells. In a

subsequent study, a proper slide culture technique with the modified filter paper was established so that it could be seen the development of mitochondria together with conidial growth simultaneously under confocal laser scanning microscopy. The results showed that as conidia growing into mature, the volume of the mitochondria decreases. Interestingly, on a particular point, mitochondria grow and develop again that has been proven with the increase of mitochondrial amount.

With this result, the mitochondrial dynamics of *P. oryzae* showed a unique behavior and required further observation by slide culture technique with more samples. Because these mitochondrial dynamics related to information about mitochondrial amount changes. In the future study, this result will help to answer how mutated mitochondria cause resistance to QoI fungicides.

REFERENCES:

1. **Affourtit C, Heaney SP, Moore AL** (2000) Mitochondrial electron transfer in the wheat pathogenic fungus *Septoria tritici* : on the role of alternative respiratory enzymes in fungicide resistance. Biochimica et Biophysica Acta 1459 : 291-298. doi:10.1016/s0005-2728(00)00157-2.
2. **Anesiadis T, Karaoglanidis S, Tzavella-Klonari K** (2003) Protective, Curative and Eradicant Activity of Strobilurin Fungicide Azoxystrobin against *Cercospora beticola* and *Erysiphe betae*. J. Phytophathology 151: 647-651. https://doi.org/10.1046/j.1439-0434.2003.00780.x
3. **Anke T, Oberwinkler F, Steglich W, Schramm G** (1977) The strobilurins-new antifungal antibiotics from basidiomycete *Strobilurus tenacellus* (Pers. ex Fr.) Sing. The Journal of Antibiotics 30 (10): 806-810. doi:10.7164/antibiotics.30.806.
4. **Ashrafi G, Schwarz TL** (2013) The pathways of mitophagy for quality control and clearance of mitochondria. Cell Death Differ. 20(1):31-42. doi: 10.1038/cdd.2012.81.
5. **Asibi AE, Chai Q, Coulter JA** (2019) Rice Blast: a disease with implications for global food security. Agronomy 9 (8), 451. https: // doi. org/ 10.3390/ agronomy 9080451
6. **Barr CM, Neiman M, Taylor DR** (2005) Inheritance and recombination of mitochondrial genomes in plants, fungi and animals. New Phytologist 168: 39-50. doi: 10.1111/j.1469-8137.2005.01492.x
7. **Buhlman L, Damiano M, Bertolin G, Ferrando-Miguel R, Lombès A, Brice A, Corti O** (2014) Functional interplay between Parkin and Drp1 in mitochondrial

fission and clearance. Biochim Biophys Acta. 1843(9):2012-2026. doi: 10.1016/j.bbamcr.2014.05.012.

8. **Bloemendal S, Kück U** (2013) Cell to cell communication plants, animals, and fungi: a comparative review. Naturwissenschaften 100: 3-19. doi 10.1007/s00114-012-0988-z.
9. **Bussaban B, Lumyong S, Lumyong P, Seelanan T, Park DC, McKenzie EHC, Hyde KD** (2005) Molecular and morphological characterization of Pyricularia and allied genera. Mycologia 97(5): 1002-1011. doi: 10.1080/15572536.2006.11832750.
10. **Calderone R, Li D, Traven A** (2015) System level impact of mitochondria on virulence : to metabolism and beyond. FEMS yeast Res 15(4):1-11. doi: 10.1093/femsyr/fov027
11. **Ebbole DJ** (2007) Magnaporthe as a model for understanding host-pathogen interaction. Annu. Rev. Phytopathol. 45: 437-456. doi:10.1146/annurev.phyto.45.062806.094346
12. **Fernández-Ortuño DF, Torés JA, de Vicente A, Perez-Garcia A** (2008) Mechanisms of resistance to QoI fungicides in phytopathogenic fungi. International Microbiology 11:1-9. doi: 10.2436/20.1501.01.38
13. **Fischer MS, Wu VW, Lee JE, O'Molley RC, Glass NL** (2018) Regulation of Cell-to-Cell Communication and Cell Wall Integrity by a Network of MAP Kinase Pathways and Transcription Factors in *Neurospora crassa*. Genetics 209 (2): 489-506. https://doi.org/10.1534/genetics.118.300904
14. **Gisi U, Sierotzki H, Cook A, McCaffery A** (2002) Mechanisms influencing the evolution of resistance to Qo inhibitor fungicides. Pest Manag Sci 58:859-867. doi: 10.1002/ps.565

15. **Goh J, Jeon J, Lee YH** (2017) ER retention receptor, MoERR1 is required for fungal development and pathogenicity in the rice blast fungus, *Magnaporthe oryzae*. Scientific Reports 7 (1): 1-14. doi:10.1038/s41598-017-01237-x.
16. **Han JH, Shin JH, Lee YH, Kim KS** (2018) Distinct roles of the YPEL gene family in development and pathogenicity in the ascomycete fungus *Magnaporthe oryzae*. Scientific resports 8(1):14461. doi: 10.1038/s41598-018-32633-6.
17. **Ishi K, Maruyama JI, Juvvadi PR, Nakajima H, Kitamoto K** (2005) Visualizing nuclear migration during conidiophore development in *Aspegillus nidulans* and *Aspergillus oryzae* : Multinucleation of conidia occurs through direct migration of plural nuclei from phialides and confers greater viability and early germination in *Aspergillus oryzae*. Biosci. Biotechnol. Biochem. 69 (4): 747-754. doi:10.1271/bbb.69.747
18. **Jones K, Jenkinson CB, Araújo MB, Zhu J, Kim RY, Kim DW, Khang CH** (2016) Mitotic stopwatch for the blast fungus Magnaporthe oryzae during invasion of rice cells. Fungal Genetic and Biology. 93: 46-49. http://dx.doi.org/10.1016/j.fgb.2016.06.002
19. **Kim KS, Lee Y-H** (2012) Gene Expression Profiling during Conidiation in the Rice Blast Pathogen Magnaporthe oryzae. PLoS ONE 7(8): e43202. doi:10.1371/journal.pone.0043202
20. **Kou Y, He Y, Qiu J, Shu Y, Yang F, Deng Y, Naqvi NI** (2019) Mitochondrial dynamics and mitophagy are necessary for proper invasive growth in rice blast. Molecular Plant Pathology 20 (8): 1147-1162. doi: 10.1111/mpp.12822

21. **Leach CM** (1980) Influence of humidity, red-infrared radiation and vibration on spore discharge by *Pyricularia oryzae*. The American Phytopathological Society 70(3): 201-205. doi: 10.1094/Phyto-70-201.
22. **Lee K, Singh P, Chung WC, Ash J, Kim TS, Hang L, Park S** (2006) Light regulation of asexual development in the rice blast fungus. *Magnaporthe oryzae*. Fungal genetic and biology 43:694-706. doi:10.1016/j.fgb.2006.04.005
23. **Lee YH, Dean RA** (1994) Hydrophobicity of contact surface induces appressorium formation in Magnaporthe grisea. FEMS Microbiol. Lett. 115, 71–75. https://doi.org/10.1111/j.1574-6968.1994.tb06616.x
24. **Lessemann SS, Schimpke S, Dunemann F, Deising HB** (2007) Mitochondrial heteroplasmy for the cytochrome *b* gene controls the levels of strobilurin resistance in the apple powdery mildew fungus *Podosphaera leucotricha* (Ell. & Ev.) E.S. Salmon. Journal of Plant Diseases Protection 113 (6):259-266.
25. **Li D, Calderone R** (2017) Exploiting mitochondria as targets for the development of new antifungals. Virulance 8 (2): 159-168. http:// dx. doi. org/ 10.1080/21505594. 2016. 1188235.
26. **Li C , Cao S, Zhang C, Zhang Y, Zhang Q, Xu JR, Wang C** (2018) MoCDC14 is important for septation during conidiation and appressorium formation in Magnaporthe oryzae. Molecular Plant Pathology 19 (2): 328-340. doi: 10.1111/mpp.12523
27. **Miki S, Matsui K, Kito H, Otsuka K, Ashizawa T, Yasuda N, Fukiya S, Sato J, Hirayae K, Fujita Y, Nakajima T, Tomita F, Sone T** (2009). Molecular cloning and characterization of the AVR-Pia locus from a Japanese field isolate of *Magnaporthe oryzae*. Mol Plant Pathol 10(3): 361–374. http://doi.org/10.1111/j.1364-3703.2009.00534.x.

28. **Osman C, Noriega TR, Okreglak V, Fung JC, Walter P** (2015) Integrity of yeast mitochondrial genome, but not its distribution and inheritance, relies on mitochondrial fission and fusion. PNAS 112 (9): E947-E956.
29. **Pennisi E** (2010) Armed and dangerous. Science. 327:804–805. doi: 10.1126/science.327.5967.804
30. **Pinnschmidt HO, Klein-Gebbinck HW, Bonman JM, Kranz J** (1993) Comparison of aerial concentration, deposition, and infectiousness of conidia of *Pyricularia grisea* by spore sampling technique. Phytopathology 83:1182-1189
31. **Potapova TV, Boitzova LJ, Golyshev SA, Popinako AV** (2011) Dynamics of Mitochondria during the *Neurospora crassa* Tip Growth. Membrane and cell biology 5 (4): 316-323.
32. **Potapova TV, Boitzova LJ, Golyshev SA, Popinako AV** (2014) The Organization of Mitochondria in Growing Hyphae of *Neurospora crassa* . Cell and Tissue Biology 8 (2): 166-174.
33. **Rafelski, S. M., Viana, M. P., Zhang, Y., Chan, Y.-H. M., Thorn, K. S., Yam, P., et al.** (2012). Mitochondrial network size scaling in budding yeast. Science 338 (6108): 822-824. http://dx.doi.org/10.1126/science.1225720.
34. **Rao KM, Jesudhas ML** (1984) Conidium ontogeny in pyricularia. Phytopath. 110 (3): 235—244.
35. **Ruf D, Brantl V, Wagener J** (2018) Mitochondrial Fragmentation in *Aspergillus fumigatus* as Early Marker of Granulocyte Killing Activity. Front Cell Infect Microbiol. 8 (128): 1-13. doi: 10.3389/fcimb.2018.00128

36. **Sica V, Izzo V, Manuel J, Pedro BS, Zamzami N, Maiuri MC** (2016) Mitophagy : sensors, regulators, and effectors In. M.A. Hayat (ed): Autophagy, Volume 9. Elsevier Inc. pp 91-104. doi: http://dx.doi.org/10.1016/B978-0-12-802936-7.00003-9

37. **Springer ML, Yanofsky C** (1989) A morphological and genetic analysis of conidiophore development in *Neurospora crassa.* Genes and Development 3: 559-571.

38. **Steinberg G, Harmer NJ, Schuster M, Kilaru S** (2017a) Woronin body-based sealing of septal pores. Fungal Genetic and Biol 109:53-55. doi: 10.1016/j.fgb.2017.10.006.

39. **Steinberg G, Schuster M, Hacker C, Kilaru S, Correja A** (2017b) ATP prevents Woronin bodies from sealing septal pore in unwounded cells of the fungus Zymoseptoria tritici. Cell Microbiol. 19(11): e12764. doi: 10.1111/cmi.12764

40. **TeBeest DO, Guerber C, Ditmore M** (2007) Rice Blast. https://www.apsnet.org/edcenter/disandpath/fungalasco/pdlessons/Pages/RiceBlast.aspx

41. **Twig G, Elorza A, Molina AJA, Mohamed H, Wikstrom JD, Walzer G, Stiles L, Haigh SE, Katz S, Las G, Alroy J, Wu M, Py BF, Yuan J, Deeney JT, Corkey BE, Shirihai OS** (2008) Fission and selective fusion govern mitochondrial segregation and elimination by autophagy. The EMBO Journal 27 (2): 433-446. doi: 10.1038/sj.emboj.7601963

42. **van Peer A, Müller WH, Boekhout T, Lugones T, Wösten HAB** (2009) Cytoplasmic Continuity Revisited: Closure of Septa of the Filamentous Fungus *Schizophyllum commune* in Response to Environmental Conditions. PLoS One 4(6): e5977. doi: 10.1371/journal.pone.0005977.

43. **Viana, MP, Lim S, Rafelski, SM.** (2015) Quantifying Mitochondrial Content in Living Cells. In E. Paluch (Ed.), Biophysical Methods in Cell Biology **125**: 77-93.

44. **Vielba-Fernández A, Bellón-Gómez D, Torés JA, de Vicente A, Pérez-García A, Fernández-Ortuño D** (2018) Heteroplasmy for the Cytochrome *b* Gene in *Podosphaera xanthii* and its Role in Resistance to QoI Fungicides in Spain. Plant Disease 102 (8) : 1599-1605. https://doi.org/10.1094/PDIS-12-17-1987-RE

45. **Wang P, Sha T, Zhang Y, Cao Y, Mi F, Liu C, Yang D, Tang X, He X, Dong J, Wu J, Yoell S, Yoell L, Zhang KQ, Zhang Y, Xu J** (2017) Frequent heteroplasmy and recombination in the mitochondrial genomes of the basidiomycete mushroom *Thelephora ganbajun*. Scientific reports 7:1626. doi:10.1038/s41598-017-01823-z

46. **Westermann B, Prokisch H** (2002) Mitochondrial dynamics in filamentous fungi. Fungal genetics and biology 36: 91-97. doi: 10.1016/S1087-1845(02)00019-1.

47. **Wilson RA, Talbot NJ** (2009) Under pressure: Investigating the biology of plant infection by *Magnaporthe oryzae*. Nature review microbiology 7: 185-195. doi:10.1038/nrmicro2032

48. **Yang J-S, Kim J, Park S, Jeon J, Shin YE, Kim S** (2013) Spatial and functional organization of mitochondrial protein network. Sci Rep 3:1403. doi: 10.1038/srep01403.

49. **Zhang Y, Shi H, Liang S, Ning G, Xu N, Lu J, Liu X, Lin F** (2015) MoARG1, MoARG5,6 and MoARG7 involved in arginine biosynthesis are essential for growth, conidiogenesis, sexual reproduction, and pathogenicity in Magnaporthe oryzae. Microbiological Research 180 : 11-12. doi: 10.1016/j.micres.2015.07.002.

50. **Zhong K, Li X, Le X, Kong X, Zhang H, Zheng X, Zheng X, Wang P, Zhang Z** (2016) MoDnm1 dynamin mediating peroximal and mitochondrial fission in complex

with MoFis1 and MoMdv1 is important for development of functional appressorium in *Magnaporthe oryzae*. Plos Pathogen 12 (8): 1-34. doi:10.1371/journal.ppat.1005823

Acknowledgments

I would like to give my sincere gratitude to this following organizations and peoples for their support which makes it possible for me to complete my study:

Indonesia Endowment Fund for Education (LPDP) for granting the scholarship to pursue this doctoral degree. Plant Protection Department, Faculty of Agriculture, The University of Brawijaya for giving me the chance and permission to study abroad.

My sincere thanks go to my supervisors, whom I will remain indebted to Professor Teruo Sone, Ph.D. and Dr. Abe Ayumi who provided me with the best academic guidance during my studies at Hokkaido University. In addition, they made the environment very comfortable for the acquisition of knowledge through their kindness, team spirit and social cohesion. I am pleased, lucky and so proud to have had them as my supervisors and future mentors.

My sincere thanks also go to my family for their sacrifice in accompanying me of living in Sapporo Japan. Especially to my lovely wife Anna Uswatun Hasanah who had to take care, my lovely kids, Mukhlis Khoiruman Tazakka and Ayumi Shofwah Najati, all of you are really a beautiful miracle and gift that was given by God in this world.

My Gratitude also goes to my friend, Pradabrat Prajanket, Dineesha Nipuni, Phyo Han Twin and all students in my Laboratory for their assistance especially in helping me get acquaintance with the laboratory.

All praise is due to Allah Almighty, only from His blessing and every best sholawat for Rosulullah SAW because of his love; finally, I could finish my doctoral study at Hokkaido University.

Muhammad Akhid Syib'li